

SDSR: A Spectral Divide-and-Conquer Approach for Species Tree Reconstruction

Ortal Reshef¹, Ofer Glassman³, Or Zuk¹, Yariv Aizenbud², Boaz Nadler³, and Ariel Jaffe¹

¹Department of Statistics and Data Science, Hebrew University of Jerusalem

²Department of Applied Mathematics, Tel Aviv University

³Department of Computer Science and Applied Mathematics, Weizmann Institute of Science

Abstract

Recovering a tree that represents the evolutionary history of a group of species is a key task in phylogenetics. Performing this task using sequence data from multiple genetic markers poses two key challenges. The first is the discordance between the evolutionary history of individual genes and that of the species. The second challenge is computational, as contemporary studies involve thousands of species. Here we present **SDSR**, a scalable divide-and-conquer approach for species tree reconstruction based on spectral graph theory. The algorithm recursively partitions the species into subsets until their sizes are below a given threshold. The trees of these subsets are reconstructed by a user-chosen species tree algorithm. Finally, these subtrees are merged to form the full tree. On the theoretical front, we derive recovery guarantees for **SDSR**, under the multispecies coalescent (MSC) model. We also perform a runtime complexity analysis. We show that **SDSR**, when combined with a species tree reconstruction algorithm as a subroutine, yields substantial runtime savings as compared to applying the same algorithm on the full data. Empirically, we evaluate **SDSR** on synthetic benchmark datasets with incomplete lineage sorting and horizontal gene transfer. In accordance with our theoretical analysis, the simulations show that combining **SDSR** with common species tree methods, such as **CA-ML** or **ASTRAL**, yields up to 10-fold faster runtimes. In addition, **SDSR** achieves a comparable tree reconstruction accuracy to that obtained by applying these methods on the full data.

1 Introduction

Species tree reconstruction from genetic data is crucial for addressing many evolutionary questions, such as diversification events, branching structures, and shared ancestry among organisms [61, 65]. Historically, species trees were inferred using genetic variations at a single marker. Common approaches for tree recovery include distance-based methods such as NJ and UPGMA [49, 50], maximum likelihood (ML) [23, 42, 45, 52], and Bayesian methods [22, 46, 64].

In recent years, advances in data acquisition have led to species tree reconstruction using sequences from multiple genetic markers [3, 34, 58, 69]. Species tree reconstruction from such data introduces two key challenges. The first is the discordance between the evolution of the species and of their genes, resulting in gene trees that may be different from each other, and from the species tree. This discordance arises from several biological phenomena [11, 18, 44, 51], with horizontal gene transfer (HGT) and incomplete lineage sorting (ILS) considered as two of the most significant contributors [19, 36, 55], see Fig. 1 for an illustration. A second challenge is scalability, as contemporary phylogenetic studies often analyze tens of thousands of species and hundreds of genes [6, 43, 70].

Several approaches were proposed for species tree reconstruction from sequences at multiple markers. Perhaps one of the simplest ones is Concatenation Analysis using Maximum Likelihood (**CA-ML**). In this approach, the gene sequences of each species are concatenated, and the species tree is recovered by maximum likelihood. Hence, **CA-ML** ignores the discordance between gene and species trees. Indeed, **CA-ML** has been shown to be statistically inconsistent under the multispecies coalescent (MSC) model [33, 47].

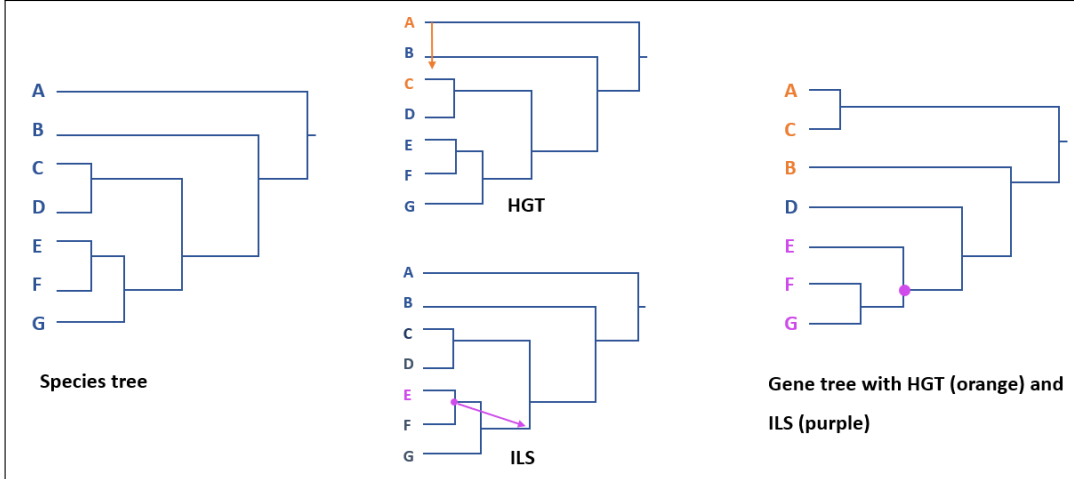


Figure 1: Discordance between a species tree and a gene tree due to one HGT event (orange) and one ILS event (purple). In HGT, a segment of genetic material is transferred horizontally from a donor species A , to a receptor species C [16, 25]. In ILS, the divergence event associated with species E occur at an earlier time in the gene tree than in the species tree [20].

A different approach to species tree reconstruction is to first estimate all the individual gene trees by some tree reconstruction method. Then, the species tree is inferred by summarizing information from all gene trees. Methods applying this approach are known as *summary methods*. Examples include *NJst* [34], *STAR* [35], *ASTRID* [58], and *ASTRAL* [37, 38, 69]. These summary methods were proven to be consistent under the MSC model, assuming the input gene trees are estimated correctly [3, 35, 37, 58]. However, errors in the inferred gene trees may have a substantial impact on the accuracy of the reconstructed species tree see [48] and [59, Ch. 10]. On the computational front, summary methods may be slow on large datasets, as they first reconstruct all the individual gene trees.

To handle datasets with thousands of species, several divide-and-conquer algorithms were developed. These methods break down the species tree reconstruction into smaller, more manageable tasks. One strategy is to randomly divide the species into overlapping subsets and construct a subtree for each subset using an existing species tree inference method. The resulting subtrees are then merged into a species tree using a supertree algorithm [27, 28, 41]. This merging operation involves NP-hard optimization problems [60], which pose limitations on the accuracy and scalability of supertree algorithms. *TreeMerge* [39, 40] partitions the species into disjoint subsets. Then, it reconstructs a subtree for each and merges them using a species dissimilarity matrix. *uDance* [7] offers an alternative divide-and-conquer strategy. It recovers a backbone tree from a subset of species and assigns each of the remaining species to an edge in the backbone tree. Then, the algorithm reconstructs a subtree for every group of species assigned to the same edge. Empirically, on simulated datasets with a large number of genes and species, *uDance* outputs quite accurate species trees. However, *uDance* has not been proven to be statistically consistent under the MSC or other models.

In this paper we present *SDSR*, a recursive divide-and-conquer method to recover a species tree from multiple gene sequences. At each step of the recursion, if the input set of species is sufficiently small, its corresponding species subtree is reconstructed by a user-chosen species tree method. Otherwise, the set of species is partitioned into two disjoint subsets. This is performed by a spectral approach, based on the Fiedler eigenvector of the average of graph Laplacian matrices for the different genes. Finally, the small trees are merged to construct the full species tree. The partitioning step builds upon and extends [1], which was designed to reconstruct a tree from a single gene alignment.

With *SDSR*, we make the following contributions:

- We prove that under the MSC model, in the limit of an infinite number of genes, *SDSR* is asymptotically consistent. Specifically, the species in each partition belong to disjoint clans in the species tree. In addition, we derive finite-sample guarantees on the number of genes required for accurate partitions. Our analysis

assumes that the Laplacian matrices of individual genes are perfectly known. This is analogous to the assumption made in the analysis of summary methods, that their gene trees are inferred without errors.

- The SDSR partitions are deterministic, which yields a simple and straightforward way to merge the subtrees into the full species tree. Moreover, if SDSR partitioned correctly the species and the subtrees were recovered correctly, the merging step is provably correct, so the output will be the exact species tree. Importantly, SDSR merging step does not require solving an NP-hard problem, unlike previous divide-and-conquer methods.
- SDSR combined with common species tree reconstruction algorithms, such as CA-ML or ASTRAL yields significant speedups compared to applying the base algorithm to reconstruct the full tree. For example, reconstructing a 200-species tree from 100 genes with SDSR + CA-ML has an 8-times faster runtime on a single CPU, while achieving accuracy similar to CA-ML on the full data. In addition, SDSR can be trivially parallelized.

The rest of the paper is organized as follows. In Section 2, we introduce the problem setting and several definitions. The SDSR algorithm is described in Section 3. Its computational complexity is analyzed in Section 4. Theoretical guarantees under the MSC model are provided in Section 5. In Section 6, we present an empirical evaluation of SDSR, in terms of accuracy and runtime, and compare it to several competing species tree methods. We conclude with a summary and discussion in Section 7.

2 Problem Setting

Let $\mathcal{T} = (V, E)$ denote an unrooted binary species tree with m terminal and $m - 2$ non-terminal nodes. Terminal nodes correspond to present-day species, whereas non-terminal nodes to ancestor species. We denote the indices of the terminal nodes by $[m] \equiv \{1, 2, \dots, m\}$ and the non-terminal nodes by $\{m + 1, \dots, 2m - 2\}$.

The observed data for each current species at a specific gene is a sequence of symbols from a set $\{\alpha_1, \dots, \alpha_\ell\}$. In the common DNA setting, $\ell = 4$ and the set is $\{A, C, G, T\}$ which are the four nucleotide bases. In the problem at hand, we are given a set of K gene alignments, denoted $\{X^g\}_{g=1}^K$. A single gene alignment $X^g \in \{\alpha_1, \dots, \alpha_\ell\}^{m \times n_g}$ contains m sequences of length n_g , where each sequence corresponds to a single species. We denote by $X_i^g = (X_{i1}^g, \dots, X_{in_g}^g)$ the sequence that corresponds to species i in the g -th gene. The goal is to reconstruct the species tree from these K gene alignments.

In this work, we present a spectral divide-and-conquer approach for species tree reconstruction. Our algorithm is based on a weighted graph, where the nodes correspond to the species, and the weights measure a specific similarity between the species. As detailed below this similarity is computed using all K gene alignments. To this end, we introduce several notations.

Similarity measure. For each gene g with gene alignment matrix X^g , we compute a measure of evolutionary distance $\hat{D}^g(i, j)$ between all pairs of observed species (i, j) . For example, a common measure is the log-determinant distance, which estimates the determinants of the transition matrices between X_i^g and X_j^g [10]. Other measures take into account varying mutation rates along the sequence [62]. Next, we compute the gene $m \times m$ similarity matrix between all m species, via

$$\hat{S}^g(i, j) = \exp(-\hat{D}^g(i, j)), \quad \forall i, j \in [m]. \quad (1)$$

Graph Laplacian and Fiedler vector. The above similarity matrix \hat{S}^g can be viewed as a weight matrix of an undirected graph G^g , whose nodes are the m observed species. Let A^g denote the diagonal matrix with entries $A^g(i, i) = \sum_{j=1}^m \hat{S}^g(i, j)$. The normalized Laplacian L^g of the similarity graph is defined by,

$$L^g = I - (A^g)^{-0.5} \hat{S}^g (A^g)^{-0.5}. \quad (2)$$

For any connected graph, the Laplacian matrix is positive semi-definite with a zero eigenvalue with multiplicity one. The Fiedler vector is the eigenvector of L that corresponds to its smallest non-zero eigenvalue.

Finally, to motivate our approach, we recall some standard definitions for trees.

Algorithm 1 SDSR

Input: Gene alignments $\{X^g\}_{g=1}^K$ for a set of species C , threshold τ , tree reconstruction subroutine, minimum partition ratio β .

Output: Reconstructed species tree.

For every gene, compute an estimated distance matrix \hat{D}^g , its similarity matrix S^g via Eq. (1), and the Laplacian L^g by Eq. (2). Then, compute the average Laplacian \bar{L} via Eq. (3).

Compute a partition C_1, C_2 of the set of species C by constrained k -means with minimum size $\beta|C|$ on the Fiedler vector of \bar{L} .

Select outgroups $O_1 \in C_1$ and $O_2 \in C_2$ and set $\tilde{C}_1 = C_1 \cup \{O_2\}$ and $\tilde{C}_2 = C_2 \cup \{O_1\}$.

for $i = 1, 2$ **do**

if $|\tilde{C}_i| > \tau$ **then**

 Apply SDSR to the subset of species \tilde{C}_i .

else

 Recover subtree \tilde{T}_i by applying the tree reconstruction subroutine to species \tilde{C}_i .

end if

end for

Let h_1 and h_2 be nodes in \tilde{T}_1 and \tilde{T}_2 connected to O_2 and to O_1 , respectively.

Remove the outgroups O_2, O_1 from \tilde{T}_1, \tilde{T}_2 .

Compute a merged tree \hat{T} by adding an edge between h_1, h_2 in the two subtrees \tilde{T}_1, \tilde{T}_2 .

return merged tree \hat{T} .

A clan and its root. A subset of nodes C in a tree \mathcal{T} is a *clan* if it can be separated from the rest of the tree by removing a single edge e . The node $h_C \in C$ that is at one end of the edge e is defined as the root of the smallest subtree that includes C . In our work, we often refer to a clan by its terminal nodes. For example, for the species tree in Figure 1, the sets of nodes (E, F) and (E, F, G) form clans in \mathcal{T} .

3 The SDSR algorithm

In this section we present our divide-and-conquer approach for recovering species trees. The input to SDSR consists of a set of K gene alignments $\{X^g\}_{g=1}^K$, a threshold τ , and a user-chosen species tree reconstruction method to recover the subtrees, which we refer to as a subroutine. The algorithm is recursive, and consists of four basic steps: (i) Partition the terminal nodes into two disjoint subsets C_1, C_2 . (ii) Add to C_2 an outgroup node $O_1 \in C_1$ and vice versa. Let $\tilde{C}_1 = C_1 \cup \{O_2\}$ and $\tilde{C}_2 = C_2 \cup \{O_1\}$. (iii) For each $i = 1, 2$, reconstruct the tree of \tilde{C}_i as follows: if $|\tilde{C}_i| > \tau$, recursively apply SDSR. Otherwise, recover its species tree by the subroutine. (iv) Merge the two subtrees computed in (iii). A pseudocode for SDSR is outlined in Alg. 1. We next describe each of the above steps, see illustration in Figure 2.

Step 1: Partitioning. For each gene g , let $\hat{S}^g(i, j)$ be the similarity between the two species i and j , computed from their gene alignments via Eq. (1). We compute a gene-Laplacian matrix L^g via Eq. (2), and the averaged Laplacian, denoted \bar{L} , by

$$\bar{L} = \frac{1}{K} \sum_{g=1}^K L^g. \tag{3}$$

We partition the species into subsets C_1, C_2 via their corresponding elements in the Fiedler vector of \bar{L} . In order to avoid extremely imbalanced partitions that do not reduce the computational complexity of the recovery problem, we apply constrained k -means [15] to the elements of the Fiedler vector. Specifically, for an input set of species C we add a constraint that the smaller subset is at least $\beta|C|$, for some value $0 < \beta < 0.5$.

Step 2: Adding outgroup nodes. As described below in step 4, the merging step relies on *outgroup rooting* [14, 24], a common approach to find the root of unrooted trees. The main idea is to reconstruct the

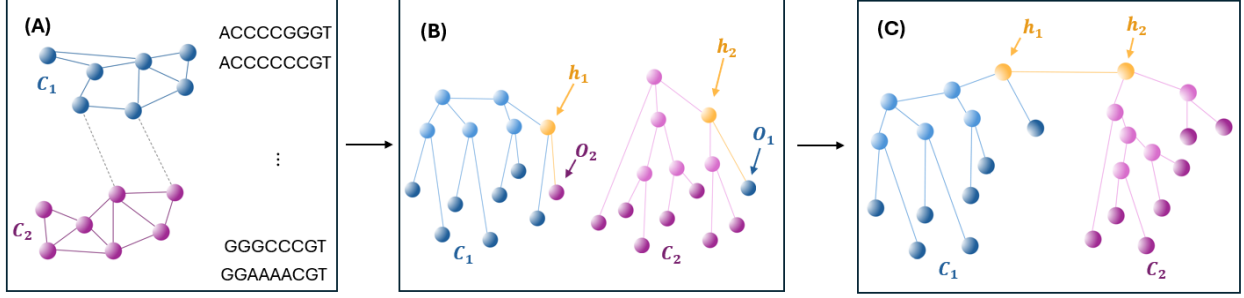


Figure 2: **SDSR workflow:** (A) Compute a graph based on the genes’ similarity matrices, where nodes represent species. The nodes are colored according to the partitions C_1, C_2 from step 1. (B) Form subsets \tilde{C}_1 and \tilde{C}_2 by adding outgroups O_2, O_1 to C_1 and C_2 , respectively, and reconstruct subtrees \tilde{T}_1 and \tilde{T}_2 . (C) The roots of the two trees are set to h_1 and h_2 , the nodes adjacent to the outgroups O_2 and O_1 . The outgroup nodes are removed, and the subtrees are merged by connecting h_1 to h_2 .

tree with an additional species, related to but outside of the species group of interest. This added species serves as a reference point for the root’s location.

In our method, outgroups are used to merge the subtrees. To this end, we add an *outgroup species* $O_2 \in C_2$ to the *ingroup species* C_1 , and vice versa. Let $\tilde{C}_1 = C_1 \cup \{O_2\}$ and $\tilde{C}_2 = C_2 \cup \{O_1\}$ be the resulting subsets. Several works showed that the selection of an outgroup may significantly impact the accuracy of the estimated root. Specifically, the distance of the chosen outgroup to the ingroup species should not be too large or too small [12, 21]. Here, we select the outgroup according to the following simple procedure. Let $v \in \mathbb{R}^m$ denote the Fiedler vector of \bar{L} computed in Eq. (3). We view distances in the Fiedler vector $|v_i - v_j|$ as indicative of distances between species i and j . We choose $O_2 \in C_2$ by looking for the species whose average distance to the species in C_1 is closest to the average of all distances from C_2 to C_1 . Namely, for each node $j \in C_2$ define $d_j = \frac{1}{|C_1|} \sum_{i \in C_1} |v_j - v_i|$ as the average distance from j to the species in C_1 and by $D(C_1, C_2) = \frac{1}{|C_2|} \sum_{j \in C_2} d_j$. Let $\bar{v}^{(2)} = \frac{1}{|C_2|} \sum_{i \in C_2} v_i$ denote the average of the elements that correspond to C_2 . By simple linear algebra

$$j = \arg \min_{j' \in C_2} |d_{j'} - D(C_1, C_2)| = \arg \min_{j' \in C_2} |v_{j'} - \bar{v}^{(2)}|.$$

The outgroup $O_1 \in C_1$ is selected in a similar way.

Step 3: Reconstruction. For each of the two subgroups \tilde{C}_1 and \tilde{C}_2 , if $|\tilde{C}_i| > \tau$, recursively call SDSR with input set \tilde{C}_i for further partitioning. Otherwise, apply a pre-selected reconstruction algorithm such as ASTRAL or NJst, to recover the (unrooted) species tree of \tilde{C}_i .

Step 4: Merging the two subtrees. The last step of SDSR is to merge the unrooted subtrees \tilde{T}_1, \tilde{T}_2 into a single tree. If the partitioning and recovery steps were accurate, then both subtrees, excluding their outgroups, form clans in the full tree \mathcal{T} . Thus, correct merging amounts to detecting for \tilde{T}_1 and \tilde{T}_2 the location of their respective root nodes. To this end, we use an outgroup approach, where the root is set to the node adjacent to the outgroup.

Let h_1, h_2 be the nodes in \tilde{T}_1, \tilde{T}_2 connected to the outgroups O_2, O_1 , respectively. In the merging step we remove the outgroups O_2, O_1 and their edges to h_1 and h_2 from \tilde{T}_1 and \tilde{T}_2 , and add an edge connecting h_1 to h_2 .

Remark 1. While the recursive structure of SDSR is similar to STDR [1], we incorporate significant changes to all of the steps in the algorithm. (i) Unlike STDR, which reconstructs a tree from a single gene alignment, SDSR addresses the challenge of tree reconstruction by merging information from multiple genes. (ii) In SDSR, we partition the species by applying constrained k -means to the Fiedler vector. This procedure often yields more accurate partitions than those obtained with the sign pattern of the Fiedler vector. (iii) In STDR, the

root was determined via a score function computed for all edges of the subtrees. The merging step in SDSR is based on an outgroup approach, which we found to be more accurate and requires fewer computations.

4 Computational complexity of SDSR

The total computational complexity of SDSR is composed of three parts: (i) the computation of K similarity matrices; (ii) the recursive partitioning and merging steps; and (iii) the recovery of the small trees via a tree reconstruction subroutine. Regarding the first part, computing K similarity matrices from gene alignments of size $m \times n$ requires $\mathcal{O}(Km^2n)$ operations.

Complexity of recursive partitioning and merging steps. Partitioning the m species requires computing the Fiedler vector of a positive semi-definite Laplacian matrix, which has a complexity of $\mathcal{O}(m^2)$ [54, Chapter 2]. Applying the outgroup approach in the merging step involves identifying the node adjacent to the outgroup in each subtree, removing the outgroup nodes, and adding a single connecting edge between the subtrees. The complexity of these operations is linear in the number of terminal nodes. Thus, the complexity of the partition and merging step *for a single iteration*, given the reconstructed subtrees, is $\mathcal{O}(m^2)$. Let $T(m)$ denote the complexity of all partitioning and merging operations. Given an input of m species, the partition satisfies $\min(|C_1|, |C_2|) \geq \beta m$, for some constant $0 < \beta \leq 0.5$. Thus, the complexity of recursively reconstructing a tree from m terminal nodes satisfies the following formula,

$$T(m) \leq \max_{\beta \leq \beta' \leq 0.5} T(\beta' m) + T((1 - \beta')m) + Cm^2, \quad (4)$$

for some constant C . By Lemma 3 in Appendix A, the complexity $T(m)$ may be bounded by

$$T(m) = \mathcal{O}(m^2),$$

where the multiplicative constant hidden in the $\mathcal{O}(\cdot)$ notation depends on β .

Complexity of reconstruction of the small trees. Given a threshold τ for the partitioning step, the smallest possible subset size is $\tau\beta$. Thus, the maximal number of subsets is bounded by $m/(\tau\beta)$. For each of these subsets we apply the user-defined tree reconstruction subroutine. Let $f(\tau)$ denote the complexity of reconstructing a tree with τ terminal nodes via the user-chosen subroutine. The complexity of reconstructing all the small trees is thus $\mathcal{O}(mf(\tau)/\tau)$.

Overall complexity of SDSR. Combining the complexity of all SDSR steps yields

$$\mathcal{O}(Km^2n) + \mathcal{O}(m^2) + \mathcal{O}\left(\frac{m}{\tau}f(\tau)\right). \quad (5)$$

In practice, the actual runtime of the first term in the expression above is negligible, and moreover it can trivially be parallelized. In addition, computing the Fiedler eigenvector is also in practice much faster than applying the tree reconstruction subroutine. Taking these points into account, let us illustrate the implications of the above formula, for a species tree reconstruction whose complexity for m species scales as $f(m) = \mathcal{O}(m^2)$. In this case, choosing $\tau = \sqrt{m}$ the complexity of the last term is $\mathcal{O}(m\sqrt{m})$, which represents a savings of $\mathcal{O}(\sqrt{m})$ as compared to applying the algorithm to the full data. In the simulation section we indeed observe runtime savings in accordance to this analysis. Next, we present a more detail comparison for CA-ML as a base routine.

Comparison to CA-ML. We compare the complexity of CA-ML to the complexity of SDSR with CA-ML as subroutine. CA-ML methods compute a local maximum of the likelihood function of the concatenated matrix by *hill climbing* iterations. The dominant factor in terms of complexity is the Subtree Pruning and Regrafting (SPR) moves, where a subtree is removed and re-attached at a different location. Testing all possible changes based on the concatenated dataset has a $\mathcal{O}(Km^2n)$ complexity for a single SPR move [5, 56]. This step is applied multiple times in many popular ML tools for tree reconstruction. In contrast, using SDSR, the cost of

reconstructing the small subtrees via ML is only $\mathcal{O}(K\tau mn)$, a reduction by a factor of m/τ . This reduction is achieved at the cost of computing the similarity, which is the dominating factor in SDSR with complexity of $\mathcal{O}(Km^2n)$. However, this operation is only done once, while SPR moves are performed multiple times in the hill-climbing process. Thus, the dominant term’s complexity is reduced from $\mathcal{O}(Km^2n)$ to $\mathcal{O}(K\tau mn)$. As illustrated in the experimental section, for datasets with 200 taxa, SDSR with CA-ML as a subroutine, is an order of magnitude faster than applying CA-ML to recover the full tree.

5 Theoretical guarantees under the multispecies coalescent model

In this section, we derive theoretical guarantees for the accuracy of the partition step of SDSR, when the number of genes is large. The guarantees are derived for a partitioning scheme that slightly differs from SDSR in two aspects: (i) it uses the unnormalized Laplacian matrices $L^g = A^g - S^g$, instead of the normalized Laplacians defined in Eq. (2). As the un-normalized L^g is linear in S^g , this allows us to first average the K similarity matrices, and then compute its corresponding Laplacian. (ii) The partitioning is determined by the sign pattern of the Fiedler vector, instead of the constrained k -means algorithm. Our analysis assumes that the un-normalized Laplacian matrices of individual genes are perfectly known. As mentioned in the introduction, this is analogous to the assumption made in the analysis of summary methods, that their gene trees are inferred without errors.

Our analysis assumes the MSC model for generating random gene trees given a species tree and the General Time Reversal (GTR) model for generating the sequence alignments given a gene tree. For our paper to be reasonably self-contained we briefly review these two probabilistic models in Section 5.1.

Our analysis consists of the following three parts:

- I In Section 5.2, we define a family of matrices $\mathcal{W}_{\mathcal{T}}$ that satisfy a *rank-1 condition* with respect to the species tree \mathcal{T} . We prove that for any graph with a weight matrix $W \in \mathcal{W}_{\mathcal{T}}$, partitioning the species according to the sign pattern of its Fiedler vector yields two clans in the species tree.
- II In Section 5.3 we present two key properties regarding the distribution of the gene trees, used in our analysis. We prove that if these properties hold, then combined with the GTR model, the expected gene similarity matrix satisfies the rank-1 condition as defined in I. Next, we show that the MSC model indeed satisfies these two condition. Hence, in the limit $K \rightarrow \infty$, partitioning the terminal nodes via SDSR yields two clans of the species tree.
- III Going beyond asymptotic consistency, in Section 5.4, we present a guarantee for correctness of the partitioning step, for a finite number of genes.

5.1 Generative models for gene trees and their sequences

In our analysis, we assume that the observed data was generated according to a combination of the following two probabilistic models. Given a species tree, we assume that the random gene trees are generated by the Multispecies Coalescent (MSC) model. Next, for each gene tree, we assume its corresponding sequences are generated by the General Time Reversal (GTR) Markov model, similar to [4]. We briefly describe these two models and then introduce the similarity measure between species, a key quantity in our analysis.

Multispecies Coalescent Model (MSC). The MSC is a common probabilistic model for gene trees given an underlying species tree. For a precise description, we refer the reader to [63, Chapter. 9] and [4]. Here, we present only the necessary details required for our analysis. We start with a definition of the species tree.

Definition 1 (Species Tree). A species tree is a binary rooted tree, $\mathcal{T} = (V, E)$, where each node h has an associated time $\tau_h \geq 0$, and each edge e has a coalescence rate $\lambda(e) > 0$. The times of the different nodes satisfy the following two properties: (1) $\tau_v = 0$ for all leaves v of the tree; (2) for each parent node h' connected by an edge to a child node h , $\tau_h < \tau_{h'}$.

By the above definition, the present time at which we observe the current species is set to $\tau = 0$. The history of species divergences is represented by the tree. Specifically, for any two species i, j , their divergence time is defined as follows. Let h_{ij} be the internal node of \mathcal{T} which is their most recent common ancestor (MRCA). This node corresponds to the divergence of the lineages i and j . The divergence time τ_{ij} of species i, j , is given by $\tau_{ij} = \tau_{h_{ij}}$. Condition (2) in the definition of the species tree above implies that divergence events in the more distant past have larger time values.

Under the MSC, a gene tree \mathcal{T}^g is randomly generated from the species tree according to the following bottom-up process. First, at time $\tau = 0$ the gene tree starts with the same set of current species as in the species tree. Then, as time progresses, the species randomly coalesce to a common ancestor at a rate determined by the species tree topology and coalescence rates $\lambda(e)$ on its edges. For any two species i, j , we denote by τ_{ij}^g their coalescence time in the gene tree \mathcal{T}^g . The coalescence process satisfies the following two conditions:

1. τ_{ij}^g is larger than τ_{ij} .
2. Their difference, denoted $\Delta_{ij}^g = \tau_{ij}^g - \tau_{ij}$, has an exponential distribution with piecewise constant rates as follows. Let h_{ij} be the MRCA of species i, j in the species tree \mathcal{T} . Let e_1, e_2, \dots, e_ℓ denote the path from h_{ij} to the root of \mathcal{T} . Then, for each branch e connecting a node h to its parent h' , conditional on not having coalesced prior to time τ_h , the coalescence rate is $\lambda(e)$. If no coalescence occurred before the root node, then beyond the root, there is a fixed rate λ_0 .

These two properties imply that the topology of the gene trees may differ from that of the species tree, see illustration in Figure 3.

Next, we describe the generative process for the observed sequences of the current species in a gene tree.

Substitution model of the sequences. We assume that the observed sequences are generated according to the the common model of sequence evolution, described by a Markov process along the edges of each gene tree (see, e.g., [63, Chapter 1]). Specifically, we assume that for a given gene tree there are substitution matrices on its edges. In addition, at each node h in the tree, there is an associated random variable $X_h \in \{\alpha_1, \dots, \alpha_d\}$. The sequence generative process begins at the root, where its state is drawn according to some initial distribution over $\{\alpha_1, \dots, \alpha_d\}$. Then, for any parent node h' connected by an edge to a child node h , the random variable X_h is drawn conditionally on $X_{h'}$ via a substitution probability matrix $P_{h|h'} \in \mathbb{R}^{d \times d}$,

$$P_{h|h'}(l, l') = \Pr(X_h = \alpha_{l'} \mid X_{h'} = \alpha_l), \quad \alpha_l, \alpha_{l'} \in \{\alpha_1, \dots, \alpha_d\}. \quad (6)$$

This process propagates from the root to the leaves. The observed sequences for each of the current species are generated by this process, independently for each location in the sequence.

As in [4], we assume the GTR model for the substitution matrices. Under this model, the sequences mutate along the edges of the tree according to a continuous-time Markov process, with a rate matrix $Q \in \mathbb{R}^{d \times d}$ that satisfies the following four properties: (i) $Q_{ij} \geq 0$ for all $i \neq j$. (ii) each row of Q sums to zero. (iii) there is a distribution vector $\pi \in \mathbb{R}^d$ with positive probabilities that satisfies $\pi Q = 0$. (iv) $\text{diag}(\pi)Q$ is symmetric. Under the GTR model, the random variable X_r at the root node r of the tree is assumed to be distributed according to π . By the first two properties above, Q is negative semi-definite, namely, all its eigenvalues are non-positive. If $Q \neq \mathbf{0}_{d \times d}$, then there is at least one eigenvalue which is strictly smaller than zero.

Next, we discuss the structure of the substitution matrices under this model. Let h, h' be two adjacent nodes in the gene tree with times $\tau_h^g, \tau_{h'}^g$. Under the GTR model with rate matrix Q , $P_{h|h'}, P_{h'|h}$ satisfy:

$$P_{h|h'} = P_{h'|h} = e^{Q|\tau_h - \tau_{h'}|}. \quad (7)$$

Using the standard identity for the matrix exponential,

$$\det(P_{h'|h}) = e^{\text{tr}(Q)|\tau_h - \tau_{h'}|}. \quad (8)$$

Note that $\text{tr}(Q) < 0$, hence Eq. (8) implies that $0 < \det(P_{h'|h}) < 1$. This condition on the determinants of the substitution matrices is known to be necessary for the identifiability of the tree topology [17].

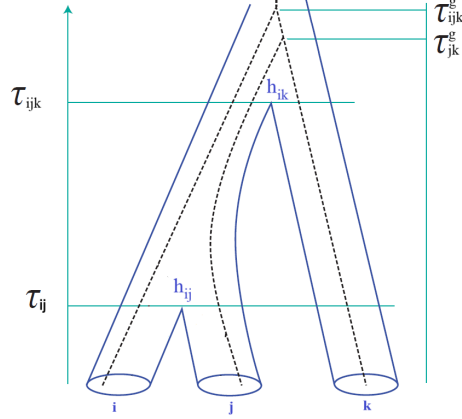


Figure 3: Example of a species tree (blue) and a realization of a gene tree (black). The vertical line is the time axis starting at $\tau = 0$ with the current species. The coalescence times in the species tree are τ_{ij} and τ_{ijk} , whereas those in the gene tree are τ_{ij}^g and τ_{ijk}^g . In this example, the gene tree and the species tree have different topologies.

We note that [4] considered a slightly more general model, allowing different rate matrices for different genes. For simplicity, in this work, we consider a fixed matrix Q for all gene trees. However, our analysis remains valid under the more general model in [4].

The similarity measure. By the Markov property, the substitution matrix $P_{i|j}^g$ between any two extant species i and j in a gene tree \mathcal{T}^g , is the product of the substitution matrices along the path between i and j . Next, note that the matrix from Eq. (1) is an estimate of the $m \times m$ *gene similarity matrix*,

$$S_{ij}^g = \det(P_{i|j}^g) \cdot \det(P_{j|i}^g), \quad (9)$$

where i and j are extant species. Under the GTR model, a closed form expression for S_{ij}^g can be derived. Recall that $\tau_i^g = \tau_j^g = 0$, and that τ_{ij}^g is the time of the MRCA of i and j in the gene tree \mathcal{T}^g . Then, by Eq.(7) and the multiplicative property of transition matrices,

$$S_{ij}^g = e^{4\text{tr}(Q)\tau_{ij}^g}. \quad (10)$$

Eq. (10) provides an explicit relation between the coalescence time of species in a gene tree and the similarity measure of their infinite length sequences. Analogously, we define the *species similarity matrix* S as follows,

$$S_{ij} = e^{4\text{tr}(Q)\tau_{ij}}, \quad (11)$$

where τ_{ij} is the coalescence time of species i and j in the species tree. Notice that $-\log(\cdot)$ of the similarity between two species gives the well-known log-determinant distance [4, 53].

We conclude this section by mentioning the multiplicativity along paths of the similarity measure. Formally, let v_1, v_2, v_3 be three nodes in a tree, such that v_2 lies on the unique path from v_1 to v_3 . We extend the definition of the similarity in Eq. (9) to a similarity function \mathcal{S} , which receives as input any pair of nodes h, h' in a tree \mathcal{T} . It is defined as follows,

$$\mathcal{S}(h, h') = \det(P_{h|h'}) \cdot \det(P_{h'|h}). \quad (12)$$

Then, the similarities of the three pairs of nodes satisfy

$$\mathcal{S}(v_1, v_3) = \mathcal{S}(v_1, v_2) \cdot \mathcal{S}(v_2, v_3). \quad (13)$$

Eq. (13) holds under the general Markov model by the Markov property together with the multiplicativity of determinants. Finally, for future use, for any edge $e = (h, h')$ in a tree we define the edge similarity as follows

$$\mathcal{S}(e) = \mathcal{S}(h, h') \quad (14)$$

Since $\text{Tr}(Q) < 0$, for each edge e the similarity $0 < \mathcal{S}(e) < 1$. For future use, we denote the lower and upper bounds of $\mathcal{S}(e)$ by δ, ξ respectively.

5.2 The species tree rank-1 condition and spectral partitioning

Let S be the similarity matrix of a species tree \mathcal{T} as defined in Eq. (11). The following theorem from [1] establishes the correctness of spectral partitioning with the graph Laplacian corresponding to S .

Theorem 1 ([1], Theorem 4.2). *Let \mathcal{T} be a binary tree, whose similarity matrix S has all entries between 0 and 1. Let v be the Fiedler vector of the Laplacian matrix of S . Let C_1, C_2 be the partition of the terminal nodes of \mathcal{T} according to the sign pattern of v . Then C_1, C_2 are clans in \mathcal{T} .*

Theorem 1 is not directly applicable for recovery of the species tree, since in our setting we do not have the species tree similarity S , but only the similarity matrices S^g of the different gene trees. Toward recovery of the species tree, we generalize Theorem 1 by introducing a set of matrices, denoted $\mathcal{W}_{\mathcal{T}}$, and proving the correctness of spectral partitioning for any weight matrix $W \in \mathcal{W}_{\mathcal{T}}$. The family $\mathcal{W}_{\mathcal{T}}$ consists of all matrices that satisfy the following two conditions.

Definition 2 (The \mathcal{T} rank-1 condition). A matrix W satisfies the rank-1 condition with respect to \mathcal{T} , if for any partition of the terminal nodes into subsets A and B , the submatrix $W(A, B) \in \mathbb{R}_+^{|A| \times |B|}$ is rank-1 if and only if A and B are clans in \mathcal{T} .

For the next condition, let $W((i, i'), (j, j')) \in [0, 1]^{2 \times 2}$ denote a submatrix of W with rows (i, i') and columns (j, j') . In addition, let \mathcal{T}_Q denote the subtree of \mathcal{T} whose terminal nodes are $Q = (i, i', j, j')$, with topology induced by \mathcal{T} .

Definition 3 (The \mathcal{T} quartet condition). A matrix $W \in [0, 1]^{m \times m}$ satisfies the quartet condition with respect to \mathcal{T} if, for every quartet of nodes $Q = (i, j, i', j')$ such that (i, j) and (i', j') are siblings in \mathcal{T}_Q ,

$$|W((i, i'), (j, j'))| > 0.$$

The following lemma, proven in Appendix B, shows that every matrix $W \in \mathcal{W}_{\mathcal{T}}$ corresponds to some tree with the same topology as \mathcal{T} .

Lemma 1. *Let $W \in \mathcal{W}_{\mathcal{T}}$ be an arbitrary matrix that satisfies the rank-1 condition and the quartet condition with respect to a tree \mathcal{T} . Then there exists an assignment of edge weights in \mathcal{T} , taking values in $[0, 1]$, such that for all pairs (i, j) , $W(i, j)$ is equal to the product of weights along the path from node i to node j .*

Lemma 1 implies that though W is not necessarily the similarity matrix of \mathcal{T} , there is a different tree $\tilde{\mathcal{T}}$, with the same topology as \mathcal{T} and different edge similarities for which W is its similarity matrix. We use this result to prove that any matrix $W \in \mathcal{W}_{\mathcal{T}}$ can be used for spectral partitioning.

Theorem 2. *Let G be a graph whose nodes correspond to the terminal nodes of a tree \mathcal{T} , and let W denote its weight matrix. Let v be the Fiedler vector of the graph's unnormalized Laplacian matrix L . If $W \in \mathcal{W}_{\mathcal{T}}$, then partitioning the terminal nodes according to the sign pattern of v yields two clans in \mathcal{T} .*

Proof. By lemma 1, if a matrix W satisfies the rank-1 condition, then there is a tree $\tilde{\mathcal{T}}$ with the same topology as \mathcal{T} such that elements $W(i, j)$ are equal to the product of edge weights of $\tilde{\mathcal{T}}$, along the path from node i to node j . Theorem 1 (Theorem 4.2 from [1]) proves that partitioning the terminal nodes according to the Fiedler vector of a graph with weights W yields two clans of $\tilde{\mathcal{T}}$. Since the topology of $\tilde{\mathcal{T}}$ is identical to that of \mathcal{T} , the partition corresponds to two clans of \mathcal{T} . \square

5.3 Asymptotic consistency of the partition step

We now prove the consistency of the partitioning step of SDSR. The proof relies on Theorem 2 combined with the following lemma, which shows that under the MSC model, the expected similarity $\mathbb{E}[S^g]$ satisfies the rank-1 condition. The proof of the lemma is in Appendix C.

Lemma 2. *Let \mathcal{T} be a species tree, and let \mathcal{T}^g be a gene tree generated according to the MSC model. Let $\mathbb{E}[S^g]$ be the expected similarity matrix over the distribution of \mathcal{T}^g . Then $\mathbb{E}[S^g]$ satisfies the rank-1 condition and the quartet condition with respect to \mathcal{T} .*

Recall that $\Delta_{i,j}^g$ denotes the difference between the coalescence time of gene g in the gene tree and the corresponding coalescence time in the species tree. For our proof of consistency we use the following two properties.

Property 1. *For any two pairs of terminal nodes, (i, j) and (i', j') , with the same MRCA in the species tree, $h_{i,j} = h_{i',j'}$, the random variables $\Delta_{i,j}^g$ and $\Delta_{i',j'}^g$ have the same distribution.*

Property 2. *For any triplet of terminal nodes $\{i, j, l\}$, where $h_{i,j}$ is the MRCA of i, j and $h_{i,l} = h_{j,l}$ is the MRCA of all three nodes, $\Delta_{i,j}^g$ is stochastically dominated by $\tau_{i,l} - \tau_{i,j} + \Delta_{i,l}^g$, such that*

$$\Pr(\tau_{i,l} - \tau_{i,j} + \Delta_{i,l}^g \geq t) > \Pr(\Delta_{i,j}^g \geq t), \quad \forall t > 0.$$

Remark 2. *Note that under the MSC model, both properties 1 and 2 above indeed hold. Indeed, property 1 holds since the distribution of $\Delta_{i,j}^g$ and $\Delta_{i',j'}^g$ is determined by the edge parameters $\lambda(e)$ on the edges between the MRCA and the root, which are the same of both pairs. As for the second property, let A be the event that the pair i, j coalesce before $\tau_{i,l}$. In that case $\Delta_{i,j}^g < \tau_{i,l} - \tau_{i,j}$. Under the condition that A did not occur, the MSC implies that the distribution of $\tau_{i,l} - \tau_{i,j} + \Delta_{i,l}^g$ is identical to that of $\Delta_{i,j}^g$. Since the probability of A is positive, we conclude that the second property holds.*

The following theorem states the consistency of the partitioning step under properties 1 and 2.

Theorem 3. *Let $\{\mathcal{T}^g\}_{g=1}^K$ be K gene trees, generated independently from a species tree according to a distribution that satisfies properties 1 and 2 above. Let $\bar{S} = \frac{1}{K} \sum_{g=1}^K S^g$ be the empirical mean of their (exact) similarity matrices S^g given in (10).*

Assume that all entries of the Fiedler vector of the Laplacian matrix corresponding to $\mathbb{E}[S^g]$ are non-zero, and that the smallest non-zero eigenvalue has multiplicity 1. Then, as $K \rightarrow \infty$, the partition computed by SDSR yields two clans in the species tree, with probability tending to one.

Theorem 3 shows that the partitioning scheme yields two clans in the limit as the number of genes $K \rightarrow \infty$. For simplicity, the theorem is stated for the case of a single (top) partition. It can, however, be applied recursively to prove consistency in multiple partitions.

5.4 Guarantee for correct partition with a finite number of genes

In the previous section, we discussed the asymptotic consistency of the partition step, as the number of genes tends to infinity. In this section, we present in Theorem 4 a guarantee for correct partitioning, which holds with high probability for a finite number of genes. For this analysis, we make the assumption that the species tree is ultrametric, that is, all its terminal nodes are at the same distance from the root. This assumption holds, for example, under the MSC+GTR model. It implies that the smallest non-zero eigenvalue of the relevant graph Laplacian matrix has multiplicity one, see [8, Lemma 7].

To present this result, we first introduce some definitions. We start by defining η , a measure of the *imbalance* at the root of the species tree \mathcal{T} . Specifically, let h_R and h_L be the two children of the root r , and let C_L and C_R be the observed species that are descendants of h_L and h_R respectively. The imbalance parameter is $\eta = \frac{\max\{|C_L|, |C_R|\}}{\min\{|C_L|, |C_R|\}}$. Next, we define \mathcal{T}_E to be the tree with the same topology as \mathcal{T} , whose similarity matrix is $\mathbb{E}[S^g]$. The existence of this tree follows from Lemma 1 combined with the fact that $\mathbb{E}[S^g] \in \mathcal{W}_{\mathcal{T}}$, as stated in Lemma 2. We denote $S_{\min} = \min_{i,j \in [m]} \mathbb{E}[S^g(i, j)]$, where the minimum is over all pairs i, j of terminal nodes. Next, we introduce a *separation parameter* s_r , which quantifies the separation between

the two clans of the first partition of \mathcal{T}_E . As above, let h_L, h_R be the two children of the root. Then, $s_r = \max\{S_E(r, h_L), S_E(r, h_R)\}$, where $S_E(h, h')$ is the similarity between two nodes $h, h' \in \mathcal{T}_E$. We are now ready to present our high-probability guarantee for correctness of the partitioning step.

Theorem 4. *Let \mathcal{T} be an ultrametric species tree with m terminal nodes and imbalance parameter η . Let h_L, h_R be the two children of the root r of \mathcal{T} and let C_L, C_R be their observed descendant species, respectively. Let $\mathcal{T}_{g=1}^K$ be K i.i.d. gene trees generated according to the MSC+GTR model, and let $\{S^g\}_{g=1}^K$ be their exact similarity matrices. Assume that for some $\epsilon > 0$, the number of genes K satisfies*

$$K \geq \begin{cases} c_1 \cdot \frac{\eta^3}{(1-s_r^2)^2 S_{\min}^2} \cdot \log\left(\frac{m}{\epsilon}\right) & \text{if } \xi \leq \frac{1}{2}, \\ c_2 \cdot \frac{\eta^3}{(1-s_r^2)^2 S_{\min}^2} \cdot m^{2+2\log_2 \xi} \cdot \log\left(\frac{m}{\epsilon}\right) & \text{if } \xi > \frac{1}{2}. \end{cases} \quad (15)$$

where c_1, c_2 are universal constants. Then, with probability larger than $1 - \epsilon$, partitioning based on the Fiedler vector corresponding to $\bar{S} = \frac{1}{K} \sum_g S^g$ yields the two clans C_L and C_R of the species tree \mathcal{T} .

Let us make several remarks regarding this theorem.

Remark 3. *Theorem 3 guarantees a correct partition into unspecified two clans. In contrast, Theorem 4 specifies that the partition is to the two clans induced by removal of the root of the tree. This more specific result is due to the assumption that the species tree is ultrametric.*

Remark 4. *As expected, as the separation parameter $s_r \rightarrow 1$, namely as the clans become poorly separated, the number of genes required to guarantee a correct partition increases to infinity.*

Theorem 4 provides a guarantee for the partitioning step of SDSR. Given that the partition is accurate, the precision of the reconstruction and merging steps depend on the outcome of the user-defined subroutine. The following proposition extends Theorem 4 by providing a theoretical guarantee for the full SDSR pipeline.

Proposition 1. *Assume that the assumptions of Theorem 4 hold, and that the number of gene alignments K satisfies Eq. (15). If, for both subsets \tilde{C}_1 and \tilde{C}_2 the subroutine computes a tree topology that matches the subtree of \mathcal{T} induced by the respective subset, then SDSR returns a tree with the same topology as \mathcal{T} , with probability $1 - \epsilon$.*

Similarly to the partitioning guarantees, Proposition 1 is written for the case of a single partition, but can be applied recursively to show a similar result for further partitions.

6 Simulations

We present an empirical evaluation of SDSR on multiple simulated datasets with ILS and HGT events. The datasets and the rates of their HGT and ILS events are described in Section 6.1. As the success of SDSR crucially depends on accurate partitioning of the species into clans, in Section 6.2 we evaluate the accuracy of this partitioning step. In Section 6.3 we evaluate the reconstruction accuracy and runtime of SDSR. For comparison, we use the following methods: (i) the RAxML maximum likelihood package [52] applied to a concatenation of the gene alignment matrices (denoted as CA-ML), and (ii) ASTRAL-IV [67, 69]. We compare the outcome of CA-ML and ASTRAL-IV to the results obtained via SDSR with these methods as subroutines for recovering small trees. Finally, on the 10,000 species repository we compare our results to uDance [7], a state-of-the-art divide-and-conquer approach for species tree reconstruction ¹.

6.1 Datasets

We considered the following three publicly available repositories. Each repository includes several datasets with a simulated species tree, a set of corresponding gene trees, and their gene alignments. These repositories have been used to evaluate species tree reconstruction methods in several previous studies.

50-species datasets. This repository consists of 100 datasets from [19], each containing 1,000 gene alignments of 50 species, with sequence length of 997bp for each gene. The first 50 datasets include only ILS

¹A python implementation of SDSR is available at <https://github.com/reshefo/sdsr>

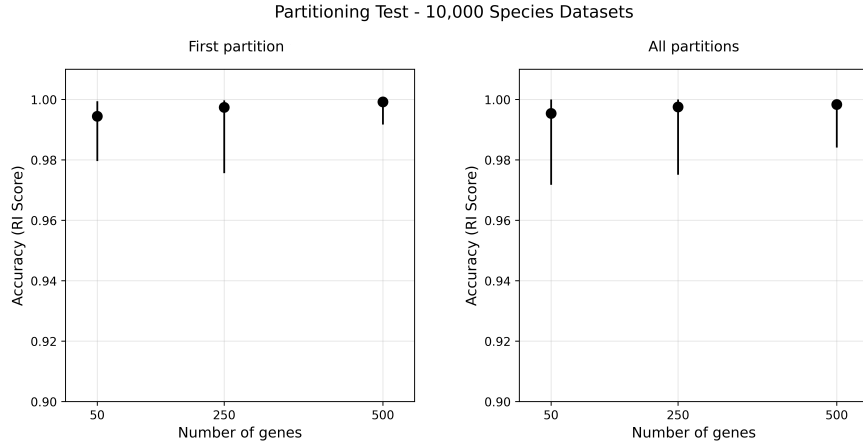


Figure 4: Partition accuracy as a function of the number of genes, on the 10,000-species datasets. Results shown for the first partition (left) and all partitions (right). The accuracy of the first partition is measured by the Rand Index similarity score to the most similar partition in the ground-truth species tree. For internal partitions, we compared the obtained partition to the most similar partition in the corresponding subtree.

events, with a mean nRF distance of 0.3 between the true gene trees and the true species tree. The other 50 datasets include, in addition to ILS events, HGT events at an average rate of 20 events per gene.

200-species datasets. This repository consists of 50 datasets from [68], each containing a simulated concatenated genome alignment of 200 species, where the simulations incorporate ILS events. As in [68], the sequence is divided into genes of size 2500bp.

10,000-species datasets. This repository consists of 10 datasets from [7], each containing 500 gene alignments. The gene sequences range in length from 169 to 869 base pairs, with an average of 406 base pairs. In this dataset, ILS and HGT rates were set such that the mean nRF distance between the species tree and gene trees was 0.03 due to ILS only and 0.44 when adding the HGT events.

6.2 Partition Accuracy

First, we evaluate the accuracy of the partitioning step of **SDSR** as a function of the number of gene alignments K for the 10,000-species datasets. The imbalance parameter β was set to 0.01 and the threshold parameter τ to 500 species. We compare the estimated partition to the most similar clan in the ground-truth species tree. Figure 4 shows the Rand Index score as a function of the number of genes. The left panel shows the score for the first partition only, and the right shows the average score for all partitions. The points mark the median of the 10 datasets, and the line is the range between the 25% and 75% quantiles. The results show that as the number of genes increases, the estimated partitions approach the ground-truth partitions. A similar experiment was done on the 50-species and 200-species repositories. The results, presented in Appendix D, show that $K = 50$ alignments were sufficient for accurate partitioning for both datasets. In addition, we compared the partitioning accuracy to a variation of our approach where the average is taken over the distance matrices instead of the similarity matrices. The results, presented in Appendix E, show that this approach yields partitions with considerably more errors than **SDSR**.

6.3 Reconstruction accuracy and runtime

We compared the accuracy and runtime of **ASTRAL** and **CA-ML** when used as stand-alone methods and when used as subroutines of **SDSR**, as a function of the number of genes. For **SDSR**, we set the imbalance parameter $\beta = 0.05$ and threshold to $\tau = 50$ species. The partition and reconstruction steps were applied to 100, 250, and 500 genes. Figure 5 shows the results for the 200-species repository. The figure shows the median accuracy and the range between the 25% and 75% quantiles of the 50 datasets in the repository. The upper row compares (i) **CA-ML**, (ii) **SDSR + CA-ML** on a single CPU, and (iii) **SDSR + CA-ML** on multiple CPUs. The

Accuracy and Runtime vs. Number of Genes – 200-Species Dataset

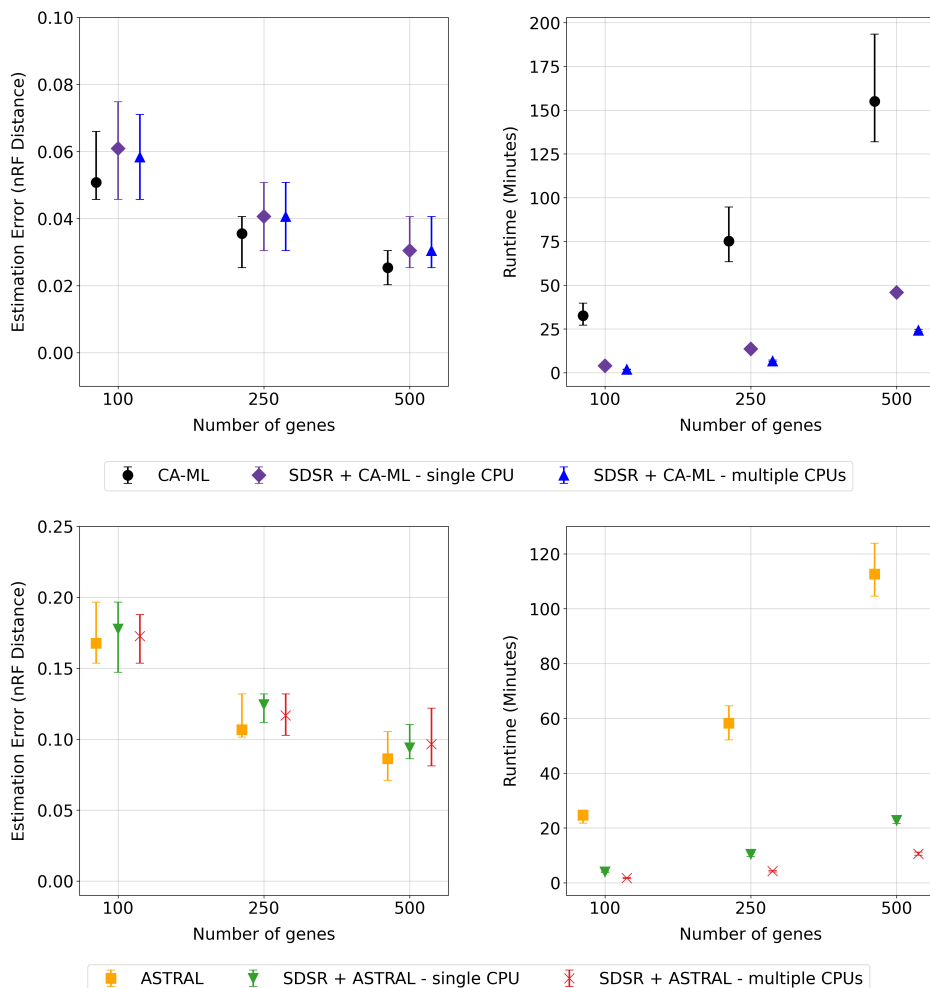


Figure 5: Accuracy and runtime as a function of the number of genes for the 200-species datasets. The upper panel presents the nRF distance between the estimated and ground truth species tree of CA-ML and SDRS using CA-ML as a subroutine. The upper right panel presents the runtime. The bottom panels present the accuracy and runtime of ASTRAL and SDRS using ASTRAL as a subroutine.

bottom row shows a similar comparison with ASTRAL. Following the original study from which the 200-species datasets were obtained [68], the input to ASTRAL was slightly different than the input to CA-ML. For ASTRAL, each gene alignment consisted of 500bp selected out of a 2,500bp window. For CA-ML, the input consisted of the entire sequences.

As seen in the figure, SDRS combined with either CA-ML or with ASTRAL, achieves similar accuracy as the respective method run as a stand-alone method to recover the full tree, while significantly reducing runtime. For example, with 100 genes, CA-ML and SDRS + CA-ML achieved similar accuracy. We note that the differences in accuracy between applying SDRS on a single and multiple CPUs are due to randomness in the RAxML method.

The runtime of SDRS + CA-ML was 8 times faster than CA-ML alone on a single CPU, and 17 times faster when all subtrees are recovered in parallel on separate CPUs. The runtime results are consistent with the analysis in Section 4. For a single CPU, the theoretical speedup of SDRS when partitioning the species to equally sized subsets is $m/\tau = 200/50 = 4$. In practice, the partition is to subsets that may be smaller than 50, which increases the speedup. For multiple CPUs, the reconstruction of the different trees is parallelized.

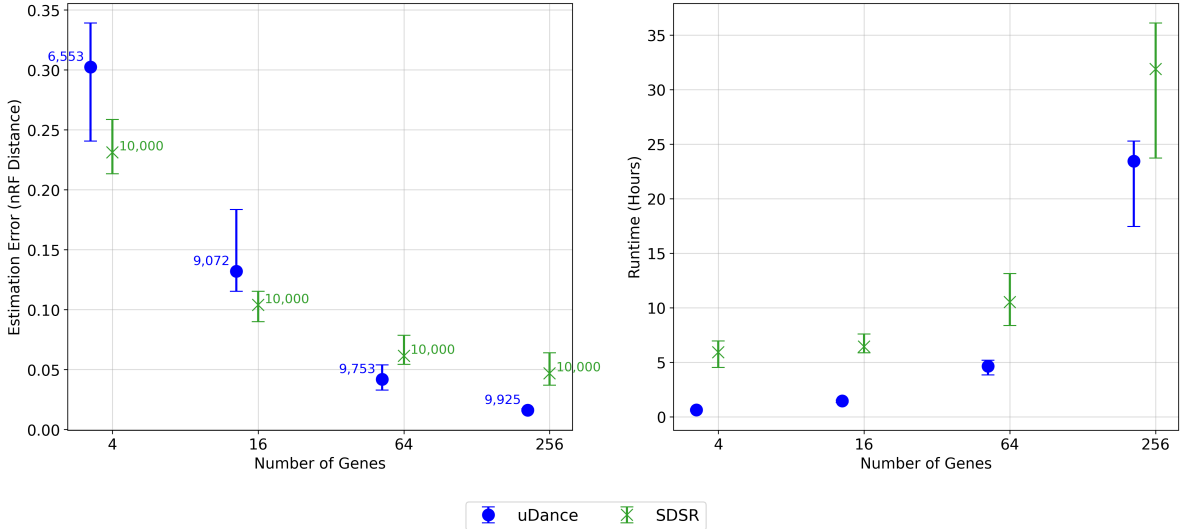


Figure 6: Comparison to `uDance` [7] on the 10,000-species datasets. The left panel shows the nRF distance between the estimated and ground-truth species tree as a function of the number of genes. Each marker represents the median runtime and nRF distance. The label on each marker denotes the median number of species in the reconstructed trees. The right panel shows the runtime of the two methods.

Hence, the theoretical speedup is the ratio between the complexity of recovering the full tree and the largest subtree, which is $m^2/\tau^2 = 16$. This is similar to the observed speedup of 17. For 500 genes, the runtime speedup is slightly reduced to 11, due to the additional time required for computing the similarity matrices.

In the Appendix section, we show the results of additional experiments that evaluate the effect of the threshold τ . First, we tested the accuracy of `SDRS` with a single partition. The results, presented in Appendix F, demonstrate that `ASTRAL` or `CA-ML` combined with `SDRS` achieves similar accuracy to the original method with reduced runtime. Next, we evaluate the effect of increasing the number of partitions by lowering the threshold parameter τ . The results, presented in Appendix G, show that using a lower threshold substantially reduces runtime while maintaining similar accuracy.

Next, we evaluate `SDRS` on larger datasets with 10,000 species. We compare our approach to `uDance` [7], a state-of-the-art divide-and-conquer approach developed for large datasets. Both methods were applied in parallel on 32 CPUs. Additionally, both methods used `ASTRAL` to reconstruct the subtrees. We set the imbalance parameter of `SDRS` to $\beta = 0.001$ and the partitioning threshold to $\tau = 1,000$. We note that for `SDRS`, partitioning was performed using all 500 genes across all runs, while reconstruction was applied with 4, 16, 64 and 256 genes. We also note that `uDance` excludes some of the species from the output tree. The average number of species in the tree computed by `uDance` was around 6,500 species for $K = 4$ genes and around 9,900 for $K = 256$. The results show that for settings where the reconstruction is done with less than $K = 64$ genes, `SDRS` computes more accurate trees than `uDance`. However, `uDance` is more accurate for cases with larger number of genes.

7 Discussion

This paper introduces `SDRS`, a discordance-aware method for species tree reconstruction. We derived theoretical guarantees under the MSC model for gene trees, and the GTR model for sequence alignments. `SDRS` can boost the scalability of many base species tree reconstruction methods. The algorithm reduces runtime even when run on a single CPU and can also be parallelized to leverage multiple CPUs. As shown in the simulations above, the time reduction achieved by our method becomes more substantial as the number of species increases.

There are several directions for future research. One potential approach to improve our method is by using

a weighted average of the gene Laplacian matrices in the partitioning step, rather than assigning equal weight to each gene. Ideally, the weight assigned to each gene would reflect its reliability, specifically, how closely its gene tree matches the species tree. Since the discrepancy between the gene trees and the species tree is generally unknown, we plan to adapt unsupervised ensemble learning methods [29, 30] that estimate reliability based on correlations among gene trees.

Another potential source of error in our approach may arise in the merging step. In the current implementation of the SDSR algorithm, a single outgroup species is used to detect the root of each subtree, after which an edge between the estimated roots connects the two subtrees. However, relying on a single outgroup may be suboptimal, as it ignores potentially informative phylogenetic signals present in additional outgroups. For finding the root of the unrooted tree, it has become common practice to use more than a single outgroup when such are available [9, 32]. In future research, we aim to add multiple outgroups to each subtree. Then, develop a machine-learning-based method for identifying the most accurate merging location among those suggested by different outgroups.

In terms of theoretical analysis, we can improve our guarantees by taking into account estimation errors in the similarity matrix. These directions can significantly increase the accuracy of our divide-and-conquer approach, enabling accurate recovery of larger trees without the need for extensive computational resources.

References

- [1] Yariv Aizenbud et al. “Spectral top-down recovery of latent tree models”. In: *Information and Inference: A Journal of the IMA* 12.3 (2023), pp. 2300–2350.
- [2] Mohamad Akra and Louay Bazzi. “On the solution of linear recurrence equations”. In: *Computational Optimization and Applications* 10.2 (1998), pp. 195–210.
- [3] Elizabeth S Allman, James H Degnan, and John A Rhodes. “Species tree inference from gene splits by unrooted STAR methods”. In: *IEEE/ACM transactions on computational biology and bioinformatics* 15.1 (2016), pp. 337–342.
- [4] Elizabeth S Allman, Colby Long, and John A Rhodes. “Species tree inference from genomic sequences using the log-det distance”. In: *SIAM journal on applied algebra and geometry* 3.1 (2019), pp. 107–127.
- [5] Elizabeth S Allman and John A Rhodes. *Lecture notes: the mathematics of phylogenetics*. Tech. rep. Tech. Rep., IAS/Park City Mathematics Institute, Park City (UT), 2005.
- [6] William J Baker et al. “A comprehensive phylogenomic platform for exploring the angiosperm tree of life”. In: *Systematic biology* 71.2 (2022), pp. 301–319.
- [7] Metin Balaban et al. “Generation of accurate, expandable phylogenomic trees with uDance”. In: *Nature biotechnology* 42.5 (2024), pp. 768–777.
- [8] Sivaraman Balakrishnan et al. “Noise thresholds for spectral clustering”. In: *Advances in Neural Information Processing Systems* 24 (2011).
- [9] Véronique Barriel and Pascal Tassy. “Rooting with multiple outgroups: consensus versus parsimony”. In: *Cladistics* 14.2 (1998), pp. 193–200.
- [10] Daniel Barry and John A Hartigan. “Asynchronous distance between homologous DNA sequences”. In: *Biometrics* (1987), pp. 261–276.
- [11] Nicholas H Barton. “The role of hybridization in evolution”. In: *Molecular ecology* 10.3 (2001), pp. 551–568.
- [12] Johannes Bergsten. “A review of long-branch attraction”. In: *Cladistics* 21.2 (2005), pp. 163–193.
- [13] Stéphane Boucheron, Gábor Lugosi, and Pascal Massart. *Concentration Inequalities: A Nonasymptotic Theory of Independence*. Oxford University Press, 2013.
- [14] Laura M. Boykin, Laura Salter Kubatko, and Timothy K. Lowrey. “Comparison of methods for rooting phylogenetic trees: A case study using Orcuttieae (Poaceae: Chloridoideae)”. In: *Molecular Phylogenetics and Evolution* 54.3 (2010), pp. 687–700.

- [15] Paul S Bradley, Kristin P Bennett, and Ayhan Demiriz. “Constrained k-means clustering”. In: *Microsoft Research, Redmond* 20.0 (2000).
- [16] Ilana Lauren Brito. “Examining horizontal gene transfer in microbial communities”. In: *Nature Reviews Microbiology* 19.7 (2021), pp. 442–453.
- [17] Joseph T Chang. “Full reconstruction of Markov models on evolutionary trees: identifiability and consistency”. In: *Mathematical Biosciences* 137.1 (1996), pp. 51–73.
- [18] James A Cotton and Roderic DM Page. “Rates and patterns of gene duplication and loss in the human genome”. In: *Proceedings of the Royal Society B: Biological Sciences* 272.1560 (2005), pp. 277–283.
- [19] Ruth Davidson et al. “Phylogenomic species tree estimation in the presence of incomplete lineage sorting and horizontal gene transfer”. In: *Genomics* 16.10 (2015), pp. 1–12.
- [20] James H Degnan and Noah A Rosenberg. “Gene tree discordance, phylogenetic inference and the multispecies coalescent”. In: *Trends in ecology & evolution* 24.6 (2009), pp. 332–340.
- [21] Rob DeSalle, Apurva Narechania, and Michael Tessler. “Multiple outgroups can cause random rooting in phylogenomics”. In: *Molecular Phylogenetics and Evolution* 184 (2023), p. 107806.
- [22] Alexei J Drummond and Andrew Rambaut. “BEAST: Bayesian evolutionary analysis by sampling trees”. In: *BMC evolutionary biology* 7 (2007), pp. 1–8.
- [23] Joseph Felsenstein. “Evolutionary trees from DNA sequences: a maximum likelihood approach”. In: *Journal of molecular evolution* 17 (1981), pp. 368–376.
- [24] Taran Grant. “Outgroup sampling in phylogenetics: severity of test and successive outgroup expansion”. In: *Journal of Zoological Systematics and Evolutionary Research* 57.4 (2019), pp. 748–763.
- [25] J. P. Hall, M. A. Brockhurst, and E. Harrison. “Sampling the mobile gene pool: Innovation via horizontal gene transfer in bacteria”. In: *Biological Sciences* 372.1735 (2017).
- [26] Roger A Horn and Charles R Johnson. *Matrix analysis*. Cambridge university press, 2012.
- [27] Daniel H Huson, Scott M Nettles, and Tandy J Warnow. “Disk-covering, a fast-converging method for phylogenetic tree reconstruction”. In: *Journal of computational biology* 6.3-4 (1999), pp. 369–386.
- [28] Daniel H Huson, Lisa Vawter, and Tandy J Warnow. “Solving large scale phylogenetic problems using DCM2.” In: *Proceedings. International Conference on Intelligent Systems for Molecular Biology*. 1999, pp. 118–129.
- [29] Ariel Jaffe, Boaz Nadler, and Yuval Kluger. “Estimating the accuracies of multiple classifiers without labeled data”. In: *Artificial Intelligence and Statistics*. PMLR. 2015, pp. 407–415.
- [30] Ariel Jaffe et al. “Unsupervised ensemble learning with dependent classifiers”. In: *Artificial Intelligence and Statistics*. PMLR. 2016, pp. 351–360.
- [31] Ariel Jaffe et al. “Spectral neighbor joining for reconstruction of latent tree models”. In: *SIAM journal on mathematics of data science* 3.1 (2021), pp. 113–141.
- [32] Tonny Kinene et al. “Rooting trees, methods for”. In: *Encyclopedia of Evolutionary Biology* (2016), pp. 489–493.
- [33] Laura Salter Kubatko and James H Degnan. “Inconsistency of phylogenetic estimates from concatenated data under coalescence”. In: *Systematic biology* 56.1 (2007), pp. 17–24.
- [34] Liang Liu and Lili Yu. “Estimating species trees from unrooted gene trees”. In: *Systematic biology* 60.5 (2011), pp. 661–667.
- [35] Liang Liu et al. “Estimating species phylogenies using coalescence times among sequences”. In: *Systematic biology* 58.5 (2009), pp. 468–477.
- [36] Wayne P Maddison and L Lacey Knowles. “Inferring phylogeny despite incomplete lineage sorting”. In: *Systematic biology* 55.1 (2006), pp. 21–30.
- [37] Siavash Mirarab et al. “ASTRAL: genome-scale coalescent-based species tree estimation”. In: *Bioinformatics* 30.17 (2014), pp. i541–i548.

- [38] Siavash Mirarab and Tandy Warnow. “ASTRAL-II: coalescent-based species tree estimation with many hundreds of taxa and thousands of genes”. In: *Bioinformatics* 31.12 (2015), pp. i44–i52.
- [39] Erin K Molloy and Tandy Warnow. “NJMerge: a generic technique for scaling phylogeny estimation methods and its application to species trees”. In: *Comparative Genomics: 16th International Conference, RECOMB-CG 2018, Magog-Orford, QC, Canada, October 9-12, 2018, Proceedings 16*. Springer, 2018, pp. 260–276.
- [40] Erin K. Molloy and Tandy Warnow. “TreeMerge: A new method for improving the scalability of species tree estimation methods”. In: *Bioinformatics* 35.14 (2019), pp. i417–i426.
- [41] Serita Nelesen et al. “DACTAL: divide-and-conquer trees (almost) without alignments”. In: *Bioinformatics* 28.12 (2012), pp. i274–i282.
- [42] Lam-Tung Nguyen et al. “IQ-TREE: a fast and effective stochastic algorithm for estimating maximum-likelihood phylogenies”. In: *Molecular biology and evolution* 32.1 (2015), pp. 268–274.
- [43] “One thousand plant transcriptomes and the phylogenomics of green plants”. In: *Nature* 574.7780 (2019), pp. 679–685.
- [44] A. C. Paquola et al. “Horizontal gene transfer building prokaryote genomes: genes related to exchange between cell and environment are frequently transferred”. In: *Journal of Molecular Evolution* 86 (2018), pp. 190–203.
- [45] Morgan N Price, Paramvir S Dehal, and Adam P Arkin. “FastTree: computing large minimum evolution trees with profiles instead of a distance matrix”. In: *Molecular biology and evolution* 26.7 (2009), pp. 1641–1650.
- [46] Bruce Rannala and Ziheng Yang. “Probability distribution of molecular evolutionary trees: a new method of phylogenetic inference”. In: *Journal of molecular evolution* 43 (1996), pp. 304–311.
- [47] Sebastien Roch and Mike Steel. “Likelihood-based tree reconstruction on a concatenation of aligned sequence data sets can be statistically inconsistent”. In: *Theoretical Population Biology* 100 (2015), pp. 56–62.
- [48] Sebastien Roch and Tandy Warnow. “On the robustness to gene tree estimation error (or lack thereof) of coalescent-based species tree methods”. In: *Systematic Biology* 64.4 (2015), pp. 663–676.
- [49] SOKAL RR. “A statistical method for evaluating systematic relationships”. In: *Univ Kans sci bull* 38 (1958), pp. 1409–1438.
- [50] Naruya Saitou and Masatoshi Nei. “The neighbor-joining method: a new method for reconstructing phylogenetic trees.” In: *Molecular biology and evolution* 4.4 (1987), pp. 406–425.
- [51] Shannon M Soucy, Jinling Huang, and Johann Peter Gogarten. “Horizontal gene transfer: building the web of life”. In: *Nature Reviews Genetics* 16.8 (2015), pp. 472–482.
- [52] Alexandros Stamatakis. “RAxML version 8: a tool for phylogenetic analysis and post-analysis of large phylogenies”. In: *Bioinformatics* 30.9 (2014), pp. 1312–1313.
- [53] Michael Steel. “Recovering a tree from the leaf colourations it generates under a Markov model”. In: *Applied Mathematics Letters* 7.2 (1994), pp. 19–23.
- [54] Gilbert W. Stewart. *Matrix Algorithms: Volume II: Eigensystems*. SIAM, 2001.
- [55] Xinxin Tan et al. “Phylogenomics reveals high levels of incomplete lineage sorting at the ancestral nodes of the macaque radiation”. In: *Molecular Biology and Evolution* 40.11 (2023), msad229.
- [56] Anastasis Togkousidis et al. “Adaptive RAxML-NG: accelerating phylogenetic inference under maximum likelihood using dataset difficulty”. In: *Molecular Biology and Evolution* 40.10 (2023), msad227.
- [57] Joel A Tropp et al. “An introduction to matrix concentration inequalities”. In: *Foundations and Trends® in Machine Learning* 8.1-2 (2015), pp. 1–230.
- [58] Pranjal Vachaspati and Tandy Warnow. “ASTRID: accurate species trees from internode distances”. In: *BMC Genomics* 16 (2015), pp. 1–13.
- [59] Tandy Warnow. *Computational phylogenetics: an introduction to designing methods for phylogeny estimation*. Cambridge University Press, 2018.

- [60] Tandy Warnow. “Divide-and-conquer tree estimation: Opportunities and challenges”. In: *Bioinformatics and Phylogenetics: Seminal Contributions of Bernard Moret* (2019), pp. 121–150.
- [61] Ping Wu et al. “TreeHub: a comprehensive dataset of phylogenetic trees”. In: *Scientific Data* 12.1 (2025), pp. 1–6.
- [62] Ziheng Yang. “Maximum likelihood phylogenetic estimation from DNA sequences with variable rates over sites: approximate methods”. In: *Journal of Molecular evolution* 39.3 (1994), pp. 306–314.
- [63] Ziheng Yang. *Molecular evolution: a statistical approach*. Oxford University Press, 2014.
- [64] Ziheng Yang and Bruce Rannala. “Bayesian phylogenetic inference using DNA sequences: a Markov Chain Monte Carlo method”. In: *Molecular biology and evolution* 14.7 (1997), pp. 717–724.
- [65] Ziheng Yang and Bruce Rannala. “Molecular phylogenetics: principles and practice”. In: *Nature Reviews Genetics* 13 (2012), pp. 303–314. DOI: 10.1038/nrg3186.
- [66] Yi Yu, Tengyao Wang, and Richard J Samworth. “A useful variant of the Davis–Kahan theorem for statisticians”. In: *Biometrika* 102.2 (2015), pp. 315–323.
- [67] Chao Zhang and Siavash Mirarab. “Weighting by gene tree uncertainty improves accuracy of quartet-based species trees”. In: *Molecular Biology and Evolution* 39.12 (2022), msac215.
- [68] Chao Zhang, Rasmus Nielsen, and Siavash Mirarab. “CASTER: Direct species tree inference from whole-genome alignments”. In: *Science* (2025), pp. 1–12.
- [69] Chao Zhang et al. “ASTRAL-III: polynomial time species tree reconstruction from partially resolved gene trees”. In: *BMC bioinformatics* 19.6 (2018), pp. 15–30.
- [70] Qiyun Zhu et al. “Phylogenomics of 10,575 genomes reveals evolutionary proximity between domains Bacteria and Archaea”. In: *Nature communications* 10.1 (2019), p. 5477.

A Complexity of partitioning and merging steps

The complexity of the partitioning and merging steps is given in its recurrence form in Sec. 4. The following lemma proves an explicit bound for this complexity.

Lemma 3. *Let $f(k)$ be a function that satisfies the recurrence equation*

$$f(k) \leq \max_{\alpha_0 \leq \alpha < 0.5} f(\alpha k) + f((1 - \alpha)k) + ck^2$$

for some $0 < \alpha_0 \leq 0.5$ independent of k . Then $f(k) = \mathcal{O}(k^2)$.

Proof. We prove the bound by induction. The induction base is trivial since for small k , there is always a constant C_c such that $f(k) \leq C_c k^2$. Assume for all $k < k_0$ we have that $f(k) \leq C_c k^2$. Then,

$$\begin{aligned} f(k_0) &\leq \max_{\alpha_0 \leq \alpha < 0.5} f(\alpha k_0) + f((1 - \alpha)k_0) + ck_0^2 \\ &\leq \max_{\alpha_0 \leq \alpha < 0.5} C_c \alpha^2 k_0^2 + C_c (1 - \alpha)^2 k_0^2 + ck_0^2 \\ &\leq k_0^2 \max_{\alpha_0 \leq \alpha < 0.5} (C_c \alpha^2 + C_c (1 - \alpha)^2 + c). \end{aligned}$$

For large enough C_c we have that $f(k_0) \leq C_c k_0^2$, which concludes the proof. \square

Remark 5. *In case the tree is split at each level with ratio constant, the computational complexity of the partitioning and merging steps can be derived directly from the Akra-Bazzi method [2].*

B Proof of Lemma 1

To prove the lemma, we first state the following auxiliary result on the rank-1 condition.

Lemma 4. *Let \mathcal{T} be a tree decomposed into $\mathcal{T} = \mathcal{T}_A \cup \mathcal{T}_B$, where A and B are clans of \mathcal{T} . Suppose that W satisfies the rank-1 condition with respect to \mathcal{T} . Then, $W(A, A)$ and $W(B, B)$ satisfy the rank-1 condition with respect to \mathcal{T}_A and \mathcal{T}_B , respectively.*

Proof of Lemma 4. Let $A = A_1 \cup A_2$ be a partition of A into two clans with respect to the tree \mathcal{T}_A . Our aim is to show that $W(A_1, A_2)$ is rank-1. To this end, note that A_1 is also a clan in the original tree \mathcal{T} . Therefore, by the rank-1 condition, $W(A_1, A_2 \cup B)$ is rank-1. This implies that its submatrix $W(A_1, A_2)$ is rank-1 as well. \square

Proof of Lemma 1. We prove the lemma by induction on the number of terminal nodes m . Our base case is a tree with two nodes x_1, x_2 where there is a single edge and a single non-diagonal element $W(1, 2)$. Hence, one can simply assign the weight $W(1, 2)$ to the edge $e(1, 2)$ and thus satisfy the lemma.

Next, we assume that the lemma holds for any tree with up to $m - 1$ terminal nodes, and prove the claim for a tree \mathcal{T} with m nodes. We partition \mathcal{T} into two rooted subtrees \mathcal{T}_A and \mathcal{T}_B by removing a single edge. Let h_A and h_B be the two root nodes of \mathcal{T}_A and \mathcal{T}_B , respectively, and let A and B be their corresponding subsets of terminal nodes, see illustration in Figure 7. Accordingly, we partition the similarity matrix W into four blocks: (i) The submatrix $W(A, A)$ which contains the pairwise similarity between nodes in A , (ii) The submatrix $W(B, B)$ which contains the pairwise similarity between nodes in B , and (iii) the matrices $W(A, B)$ and $W(B, A) = W(A, B)^T$ that contain similarities between nodes in A and those in B .

The four blocks of S satisfy the following two properties with respect to the tree \mathcal{T} .

I The submatrix $W(A, B)$ is rank-1.

II The submatrices $W(A, A), W(B, B)$ satisfy the rank-1 condition with respect to the trees \mathcal{T}_A and \mathcal{T}_B respectively.

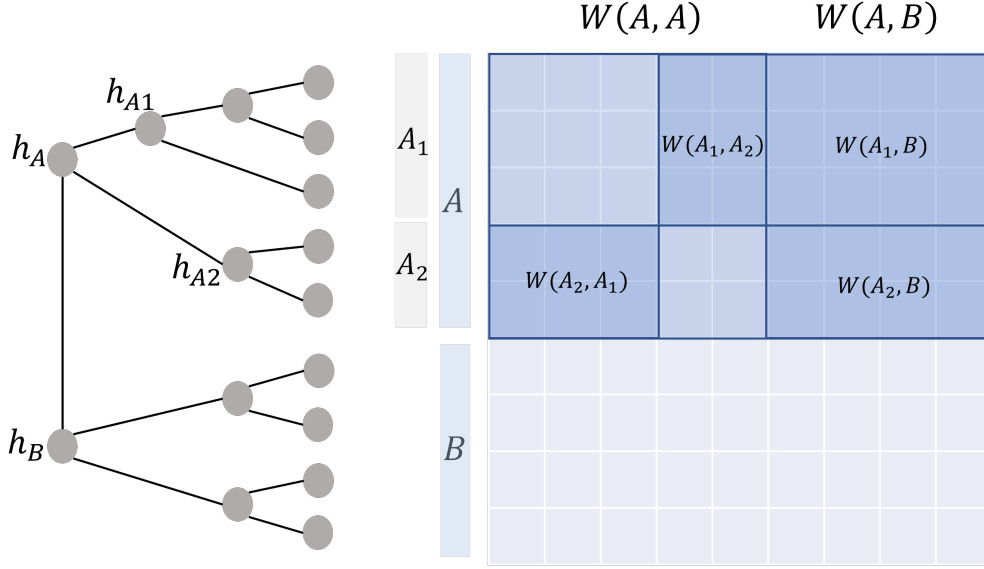


Figure 7: A tree \mathcal{T} and its corresponding similarity matrix S . On the right - the matrix block partitions used in the proof of lemma 1

Property I follows from the fact that A and B are clans of \mathcal{T} , and that by the assumption of the lemma W satisfies the rank-1 condition with respect to \mathcal{T} . Hence there are vectors v_A, v_B such that

$$W(A, B) = v_A v_B^T \quad (16)$$

Property II follows from the above auxiliary Lemma 4.

By Property II and the induction hypothesis, we can set weights to the edges of \mathcal{T}_A such that each element $W(i, j)$ where $(i, j) \in A$ equals the product of weights along the path between nodes x_i and x_j . Similarly, we can set such weights to T_B .

We denote by $w(A, h_A) \in \mathbb{R}^{|A|}$ a vector whose entries are the product of weights along the paths between the subset of nodes A and h_A . Similarly, let $w(B, h_B) \in \mathbb{R}^{|B|}$ be denote the product of weights between the subset B and h_B . Our proof is based on the following auxiliary lemma.

Lemma 5. *The vectors $w(A, h_A)$ and $w(B, h_B)$ are proportional to v_A and v_B defined in Eq. (16). Namely,*

$$w(A, h_A) = c_A v_A, \quad w(B, h_B) = c_B v_B,$$

for some constants c_A and c_B .

Lemma 5 relates properties I and II. For an arbitrary partition A, B , the singular vectors of the rank-1 submatrix $W(A, B)$ are proportional to the weights $w(A, h_A)$ and $w(A, h_B)$. We first complete the proof of Lemma 1 assuming Lemma 5 is correct. We set the weight $w(h_A, h_B) = c_A c_B$. Thus,

$$w(A, h_A) w(h_A, h_B) w(h_B, B) = w(A, h_A) c_A c_B w(h_B, B) = v_A v_B^T = W(A, B).$$

Finally, we prove that the product $c_A c_B$ is smaller than 1. Consider a quartet of nodes $(i, j) \in A$ and $(i', j') \in B$ and consider the determinant of the following submatrix

$$\left| \begin{pmatrix} W(i, j) & W(i, j') \\ W(i', j) & W(i', j') \end{pmatrix} \right| = \left| \begin{pmatrix} w(i, h_A) w(h_A, j) & w(i, h_A) c_A c_B w(h_B, j') \\ w(j, h_A) c_A c_B w(h_B, i') & w(i', h_B) w(h_B, j') \end{pmatrix} \right| = W(i, j) W(i', j') (1 - (c_A c_B)^2).$$

By the definition of the rank-1 matrix, we have that the determinant is positive, which implies that $c_A c_B < 1$. Together with property II, we found a set of weights such that $W(i, j) = w(x_i, x_j)$ for all pairs (i, j) which proves Lemma 1.

Let us now prove auxiliary Lemma 5. Let h_{A_1}, h_{A_2} and h_{B_1}, h_{B_2} be two pairs of nodes adjacent to h_A and h_B , respectively. We denote by A_1, A_2 a partition of A according to the nodes closer to h_{A_1} and h_{A_2} , see illustration in Figure 7. Consider the submatrix $W(A_1, A_2)$. By property II, we can set weights to \mathcal{T}_A such that,

$$W(A_1, A_2) = w(A_1, h_A)w(h_A, A_2) = w(A_1, h_{A_1})w(h_{A_1}, h_A)w(h_A, h_{A_2})w(h_{A_2}, A_2). \quad (17)$$

Note that we have a degree of freedom in the choice of $w(h_{A_1}, h_A)$ and $w(h_A, h_{A_2})$ since multiplying one and dividing the other by a constant does not change the product of weights between any pair of nodes in A . We will use this degree of freedom shortly.

Next, consider three submatrices: $W(A_1, A_2)$, $W(A_1, B)$ and their concatenation $W(A_1, A_2 \cup B)$. All three submatrices are rank-1, $W(A_1, A_2)$ by Eq. (17), and $W(A_1, B)$ and $W(A_1, A_2 \cup B)$ since the matrices $W(A, A)$ and W satisfy the rank-1 condition with respect to \mathcal{T}_A and \mathcal{T} , respectively. Since $W(A_1, A_2 \cup B)$ is a concatenation of $W(A_1, A_2)$ and $W(A_1, B)$, it implies that all three submatrices have the same left singular vector. By Eq. (17) this singular vector is proportional to $w(A_1, h_{A_1})$. We can apply a similar reasoning with the three matrices $W(A_2, A_1)$, $W(A_2, B)$ and $W(A_2, A_1 \cup B)$ to conclude that the left singular vector of all three matrices is proportional to $w(A_2, h_{A_2})$. We thus conclude that there are two constants c_{A_1} and c_{A_2} such that the left singular vector of $W(A_1, B)$ is equal to $c_{A_1}w(A_1, h_{A_1})$ and the left singular vector of $W(A_2, B)$ is equal to $c_{A_2}w(A_2, h_{A_2})$.

The submatrix $W(A, B)$ is a concatenation of $W(A_1, B)$ and $W(A_2, B)$. Its left singular vector v_A is thus a concatenation of $c_{A_1}w(A_1, h_{A_1})$ and $c_{A_2}w(A_2, h_{A_2})$. Recall that we have a degree of freedom for the choice of $w(h_{A_1}, h_A)$ and $w(h_{A_2}, h_A)$. We set the two weights such that

$$w(h_{A_1}, h_A)c_{A_1} = w(h_{A_2}, h_A)c_{A_2} \equiv c_A.$$

With these weights, v_A is a concatenation of $c_A w(A_1, h_A)$ and $c_A w(A_2, h_B)$, which equals $c_A w(A, h_A)$. A similar reasoning yields that $v_B = c_B w(B, h_B)$ which concludes the proof. \square

C Proof of Theorem 3

C.1 Proof of Lemma 2: $\mathbb{E}[S^g]$ satisfies the rank-1 and quartet conditions.

Proof of Lemma 2. Let $S(A, B)$ and $S^g(A, B)$ denote two similarity matrices between nodes in a subset A and nodes in the complementary subset B in the species tree and gene tree, respectively. In the following proof we first assume that A and B are clans, and hence by Lemma 3.1 in [31] $S(A, B)$ is rank-1. We prove that in this case, $\mathbb{E}[S^g(A, B)]$ is also rank-1. Then, we show that if A is not a clan, then $\mathbb{E}[S^g(A, B)]$ is not rank-1.

Assume A and B are clans obtained by disconnecting the edge between h_A and its parent node, and let $i \in A, k \in B$ be a pair of nodes with similarity $S^g(i, k)$ in the gene tree. By Eq. multiplicity of the similarity

$$S^g(i, k) = \exp(-D^g(i, k)) = \exp(-D(i, k) - 2\Delta_{ik}) = S(i, k) \exp(-2\Delta_{ik}). \quad (18)$$

Since k is external to the clan A , all pairs that include a node $i \in A$ and node k share the same common ancestor, i.e. $h_{i,k} = h_{A \cup \{k\}}$ for any $i \in A$. Thus, by property 1, the distributions of $\Delta_{i,k}$, and hence the expectation $\mathbb{E}[\exp(-2\Delta_{i,k})]$ are the same for any node $i \in A$.

Let $S(A, k)$ be a single column in $S(A, B)$ that contains the similarity values between k and the subset A in the species tree, and let $\mathbb{E}[S^g(A, k)]$ denote the expectation of the corresponding column in the gene tree. Eq. (18) implies that $\mathbb{E}[S^g(A, k)]$ is equal, up to a multiplicative factor, to $S(A, k)$. The same holds for any node $k' \in B$. Since $S(A, B)$ is rank 1, then $\mathbb{E}[S^g(A, B)]$ is also rank-1.

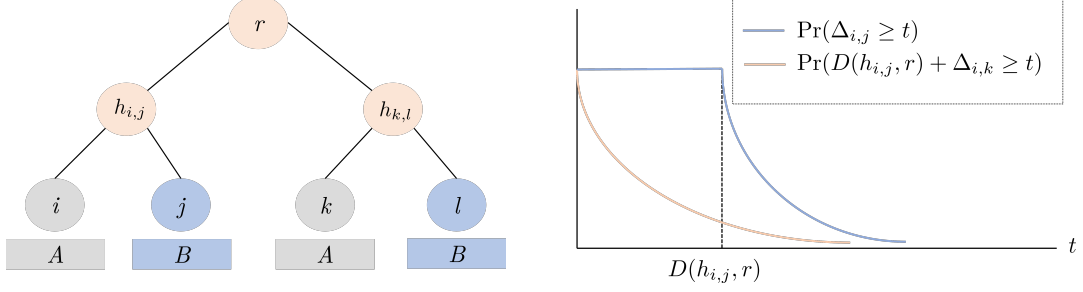


Figure 8: Left: Illustration of a quartet tree. For part (b) of our proof, we show that if A and B are not clans, $S(A, B)$ is not rank 1. Right: key property II: The random variable $\Delta_{i,k} + D(h_{i,j}, r)$ stochastically dominates $\Delta_{i,j}$.

Next, consider the case where the subset A is not a clan in the species tree. There are at least two pairs $(i, k) \in A$ and $(j, l) \in B$ where (i, j) and (k, l) are siblings in the inner structure of the quartet in the species tree, see illustration in Fig. 8. We denote by r the MRCA of the quartet. Consider the 2×2 submatrix $\mathbb{E}[S^g(A, B)]$,

$$\mathbb{E} \left[S^g((i, k), (j, l)) \right] = \begin{pmatrix} \mathbb{E}[S^g(i, j)] & \mathbb{E}[S^g(i, l)] \\ \mathbb{E}[S^g(k, j)] & \mathbb{E}[S^g(k, l)] \end{pmatrix} \quad (19)$$

Similar to Eq. (18), each element of this matrix can be expressed in the following form:

$$\mathbb{E}[S^g(i, j)] = S(i, j) \mathbb{E}[\exp(-2\Delta_{ij})].$$

In addition, by the multiplicativity property of the similarity measure we have

$$\begin{aligned} S(i, l) &= S(i, h_{i,j}) \exp(-D(h_{i,j}, r)) \exp(-D(r, h_{k,l})) S(h_{k,l}, l), \\ S(k, j) &= S(k, h_{k,l}) \exp(-D(h_{k,l}, r)) \exp(-D(r, h_{i,j})) S(h_{i,j}, j). \end{aligned}$$

Thus,

$$S(i, l)S(k, j) = S(i, j)S(k, l) \exp(-2D(h_{i,j}, r)) \exp(-2D(h_{k,l}, r))$$

The determinant of the submatrix in Eq. (19) equals,

$$\begin{aligned} & \mathbb{E}[S^g(i, j)] \mathbb{E}[S^g(k, l)] - \mathbb{E}[S^g(i, l)] \mathbb{E}[S^g(k, j)] \\ &= S(i, j)S(k, l) \left(\mathbb{E}[\exp(-2\Delta_{i,j})] \mathbb{E}[\exp(-2\Delta_{k,l})] \right. \\ & \quad \left. - \mathbb{E}[\exp(-2(D(h_{i,j}, r) + \Delta_{i,l}))] \mathbb{E}[\exp(-2(D(h_{k,l}, r) + \Delta_{k,j}))] \right) \end{aligned} \quad (20)$$

Consider the triplet (i, j, l) . The root node r is an ancestor of $h_{i,j}$ and hence by property 2 it holds that $D(h_{i,j}, r) + \Delta_{i,l}$ stochastically dominates $\Delta_{i,j}$. Since $\exp(-2d)$ is a monotonically decreasing function in d , then

$$\mathbb{E}[\exp(-2(D(h_{i,j}, r) + \Delta_{i,l}))] < \mathbb{E}[\exp(-2\Delta_{i,j})].$$

Similarly,

$$\mathbb{E}[\exp(-2(D(h_{k,l}, r) + \Delta_{k,j}))] < \mathbb{E}[\exp(-2\Delta_{k,l})].$$

Hence, the determinant of the submatrix is positive, which implies it is rank-2. Thus, $\mathbb{E}[S^g(A, B)]$ cannot be rank-1.

To prove that the quartet condition holds, it suffices to show that this condition is satisfied in any similarity matrix of a tree, whose weights are between 0 and 1. Consider a quartet $Q = ((i, j), (k, l))$ such that (i, k) and (j, l) are siblings in \mathcal{T}_Q , see Fig. 8. We denote by $S(h_{i,j}, h_{k,l})$ the similarity between the ancestor $h_{i,j}$ of (i, j) and the ancestor $h_{k,l}$ of (k, l) . The determinant $|S((i, j), (k, l))|$ is equal to,

$$|S((i, j), (k, l))| = S(i, k)S(j, l) - S(i, l)S(j, k) = S(i, k)S(j, l)(1 - S(h_{i,j}, h_{k,l})^2).$$

Since $0 < S(h_{i,j}, h_{k,l}) < 1$, the quartet is positive. \square

Partitioning Test - Single Iteration

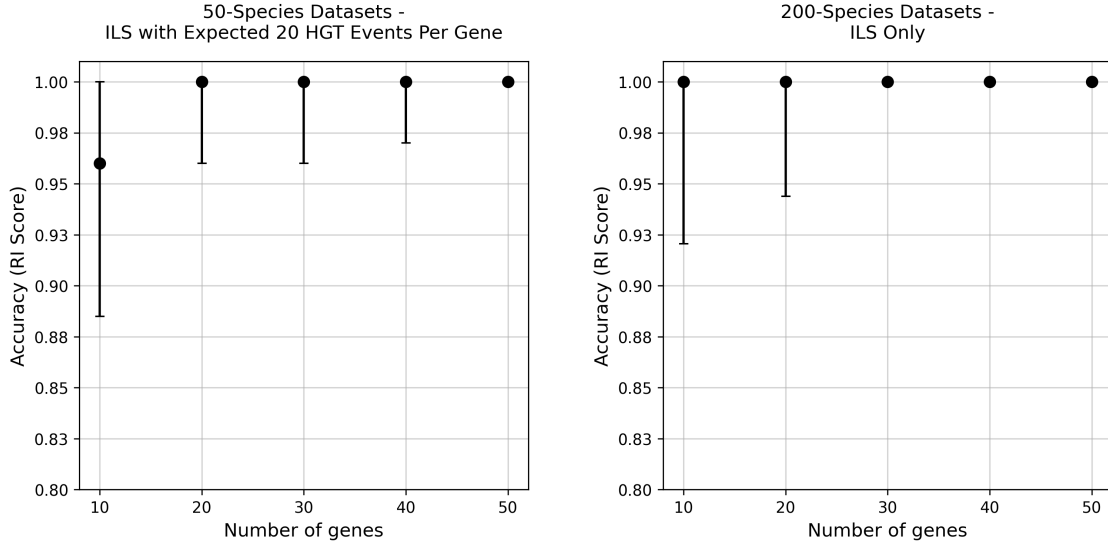


Figure 9: Accuracy of the first partition as a function of the number of genes, on the 50-species datasets (left) and the 200-species datasets (right). The accuracy is measured by the Rand Index similarity score between the partition obtained by the Fiedler vector and the most similar partition in the ground-truth species tree.

C.2 Proof of Theorem 3

Proof of Theorem 3. By Lemma 2, $\mathbb{E}[S^g]$ satisfies the rank-1 condition with respect to \mathcal{T} , namely $\mathbb{E}[S^g] \in \mathcal{W}_{\mathcal{T}}$. Let v denote the Fiedler vector of a graph whose weight matrix is equal to $\mathbb{E}[S^g]$. Since $\mathbb{E}[S^g] \in \mathcal{W}_{\mathcal{T}}$, Theorem 2 implies that partitioning the species according to v yields two clans.

Let \bar{L} be the Laplacian of a graph whose weight matrix equals the sample mean $\bar{S} = \frac{1}{K} \sum_{g=1}^K S^g$. We denote by \hat{v} the corresponding Fiedler vector, and by $0 = \gamma_1 < \gamma_2 < \gamma_3$ the smallest eigenvalues of \bar{L} . By the Davis-Kahan theorem [66],

$$\|\hat{v} - v\| \leq 2^{3/2} \frac{\|\bar{L} - \mathbb{E}[\bar{L}]\|}{\min(\gamma_2, \gamma_3 - \gamma_2)}. \quad (21)$$

By the law of large numbers \bar{S} converges to $\mathbb{E}[S^g]$, and hence \bar{L} to $\mathbb{E}[\bar{L}]$. Thus, the Davis-Kahan bound (r.h.s of Eq. (21)) converges to zero for $K \rightarrow \infty$. Since by assumption $\min_j |v(j)| > 0$, the sign pattern of \hat{v} is the same as v once the Davis-Kahan bound falls below $\min_j |v(j)|$. Thus, partitioning the terminal nodes according to the sign pattern of \hat{v} yields the same subsets as that of v , and is guaranteed to yield two clans in the species tree. \square

D Evaluating the partitioning step on the 50-species and 200-species datasets

Here, we evaluate the accuracy of the partitioning step of SDSR as a function of the number of gene alignments K for the 50-species and 200-species datasets. Recall that the parameter β sets the minimum partition in the constrained K-means. For both the 50-species and the 200-species datasets, β was set to 0.05. The threshold parameter τ was set to 50 for the 200-species datasets and to 25 for the 50-species datasets. We compare the outcome of the first partition to the most similar partition in the species tree. Figure 9 shows the Rand Index score as a function of the number of genes. The points mark the median of the 50 datasets, and the line is the range between the 25% and 75% quantiles. The results show that a small number of genes is sufficient to obtain an accurate partition for these datasets.

Partitioning Test by Distance Matrices - Single Iteration

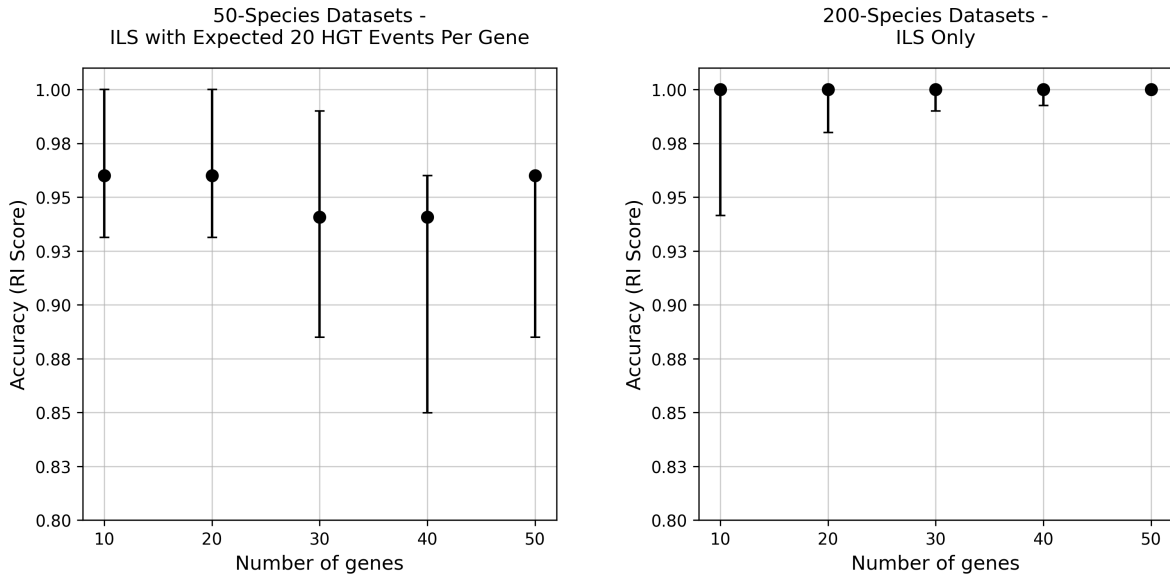


Figure 10: Accuracy of the first partition, based on distance matrices, as a function of the number of genes. (left) 50-species dataset; (right) 200-species dataset. The accuracy is measured by the Rand Index similarity score between the partition obtained by the Fiedler vector and the most similar partition in the ground-truth species tree.

E Test partitioning via average distance matrix

As described in Section 3, the SDSR partitioning approach computes a similarity matrix from each gene alignment. Here, we explore an alternative approach that is based on an average distance matrix. Let D^g denote a pairwise distance matrix estimated from the g -th gene alignment, and let \bar{D} denote the average distance matrix:

$$\bar{D} = \frac{1}{K} \sum_{g=1}^K D^g.$$

We compute a single similarity matrix via,

$$S(i, j) = \exp(-\bar{D}(i, j)),$$

and compute its corresponding Laplacian. Partitioning is then performed based on the Fiedler vector, as described in Step 1a of Section 3. To evaluate the performance of this approach, we conduct experiments on the 50 and 200 species datasets. Gene lengths and parameter values for β and τ are as described in Section D. Figure 10 presents the Rand Index score as a function of the number of genes. The points mark the median of the 50 datasets, and the line represents the range between the 25% and 75% quantiles. The results show that partitions obtained via the distance-based approach are less accurate than those obtained using the averaged Laplacian approach.

F Reconstruction accuracy with a single SDSR iteration

We compared the accuracy and runtime of ASTRAL and CA-ML when used as stand-alone methods and when used as subroutines of SDSR with a single iteration, single CPU, and $\beta = 0.05$. The experiment was conducted on the 50 and 200 species datasets. Figure 11 shows the accuracy and runtime for all methods as a function of the number of genes for the 50 species datasets. The markers represent the median, and

the lines show the range between the 25% and 75% quantiles. For a large number of genes, there is almost no difference between the accuracy of ASTRAL and SDRS + ASTRAL, and between CA-ML and SDRS + CA-ML. However, the spectral approach demonstrates a significant reduction in runtime. For instance, for the ILS-only datasets with 250 genes, the processing time of SDRS + CA-ML was around 40% of that of CA-ML.

G Reconstruction accuracy with different threshold values

Here, we measure the effect of τ , the threshold parameter that upper bounds the size of the tree partitions, on the accuracy and runtime. The experiment was conducted using the 200 species datasets. We applied CA-ML as a stand-alone method and as a subroutine within SDRS on a single CPU, using $\beta = 0.05$, and various values of τ . Figure 13 shows the runtime and accuracy vs. the number of genes. The lines mark the range between the 25% and 75% quantiles, and the markers represent the median. For lower values of τ , the spectral approach has a significantly lower runtime, with a similar accuracy.

H Proofs for the finite genes guarantee

This section is dedicated to the proof of Theorem 4, and it is organized as follows. In H.1 we prove Theorem 4 based on Lemma 6, which proved based on lemmas 8 and 9 in Subsection H.2. Then Lemma 8 and Lemma 9 proved in subsections H.3 and H.4, respectively. Finally, several auxiliary lemmas used in H.4 were proved in H.5.

H.1 Proof of Theorem 4

We first present two auxiliary results, Lemma 6 and Lemma 7. To state Lemma 6, we first introduce *the allowed error* $\Delta(\mathcal{T}_E)$, where \mathcal{T}_E is a tree with the same topology as \mathcal{T} and with similarity $\mathbb{E}[S^g]$ as discussed in Subsection 5.4. The quantity $\Delta(\mathcal{T}_E)$ is given by

$$\Delta(\mathcal{T}_E) = \frac{\sqrt{m} \cdot S_{\min}}{\sqrt{\eta} 2^{3/2} (\sqrt{m} + 1)} \min \left\{ 1, \frac{1}{1 + \eta} \left(\frac{1}{s_r^2} - 1 \right) \right\}, \quad (22)$$

where the quantities η , S_{\min} and s_r were all defined in Subsection 5.4.

The next lemma, proved in Subsection H.2, states that if the number of genes is larger than a quantity that depends on $\Delta(\mathcal{T}_E)$, then spectral partition yields two clans of the species tree. In what follows, $\|S\|$ is the spectral norm of the matrix S .

Lemma 6. *Let \mathcal{T} be an ultrametric species tree with m terminal nodes and similarity matrix S . Let h_L, h_R be the two children of the root r of \mathcal{T} and let C_L, C_R be their observed descendant species, respectively. Let $\{\mathcal{T}^g\}_{g=1}^K$ be K i.i.d. gene trees generated according to the MSC+GTR model, and let $\{S^g\}_{g=1}^K$ be their exact similarity matrices. Assume that for some $\epsilon > 0$*

$$K \geq \left(\frac{\|S\|^2}{2\Delta^2(\mathcal{T}_E)} + \frac{2\|S\|}{3\Delta(\mathcal{T}_E)} \right) \cdot \log \left(\frac{2m}{\epsilon} \right), \quad (23)$$

then, with probability larger than $1 - \epsilon$, partitioning based on the Fiedler vector corresponding to $\bar{S} = \frac{1}{K} \sum_g S^g$ yields the two clans C_L and C_R of the species tree \mathcal{T} .

The lower bound (23) depends on $\|S\|$. Next, we upper bound this quantity. Since all entries $S(i, j) \in [0, 1]$, a trivial bound is $\|S\| \leq m$. In the following lemma, proved in Appendix H.5, we present a sharper bound. To describe it, recall the definition of ξ as the upper bound on the similarity between adjacent nodes.

Lemma 7. *Let \mathcal{T} be a (rooted or unrooted) binary tree with m terminal nodes, and let S denote its associated similarity matrix. Assume that for some constant $\xi < 1$, the similarity values $S(e)$ at all edges e of \mathcal{T} satisfy $S(e) \leq \xi$. Then,*

$$\|S\| \leq \begin{cases} 3/2 & \xi \leq 0.5 \\ 1 + 2(m-1)^{1+\log_2 \xi} & \xi > 0.5 \end{cases} \quad (24)$$

With these two results, we now prove Theorem 4.

Proof of Theorem 4. Assume that the conditions of Theorem 4 hold, and in particular that the number of genes K satisfies Eq. (15). To prove the corollary, it suffices to show that the right-hand side of (23) is smaller than that of (15). Since the RHS of Eq. (23) depends on $\|S\|/\Delta(\mathcal{T}_E)$, we separately upper bound $\|S\|$ and $\frac{1}{\Delta(\mathcal{T}_E)}$.

To bound $\frac{1}{\Delta(\mathcal{T}_E)}$, we take the reciprocal of Eq. (22),

$$\frac{1}{\Delta(\mathcal{T}_E)} = \frac{\sqrt{\eta} \cdot 2^{3/2}(\sqrt{m} + 1)}{\sqrt{m}} \cdot (S_{\min})^{-1} \cdot \max \left\{ 1, (1 + \eta) \cdot \frac{s_r^2}{1 - s_r^2} \right\}. \quad (25)$$

Next, we bound the maximum term in (25). Since $\eta > 1$ and $s_r < 1$,

$$\max \left\{ 1, (1 + \eta) \cdot \frac{s_r^2}{1 - s_r^2} \right\} \leq \frac{1 + \eta}{1 - s_r^2}. \quad (26)$$

Now, notice that $\frac{\sqrt{\eta} \cdot 2^{3/2}(\sqrt{m} + 1)}{\sqrt{m}} \leq c\sqrt{\eta}$ for some constant c . Inserting this inequality and Eq. (26) into Eq. (25) gives

$$\frac{1}{\Delta(\mathcal{T}_E)} \leq c_1 \frac{\eta^{3/2}}{(1 - s_r^2)S_{\min}}, \quad (27)$$

where c_1 is some constant.

We now proceed to bounding the spectral norm $\|S\|$. By Equation (24) of Lemma 7,

$$\|S\| \leq \begin{cases} 3/2 & \text{if } \xi \leq \frac{1}{2}, \\ c_2 \cdot m^{1 + \log_2 \xi} & \text{if } \xi > \frac{1}{2}. \end{cases} \quad (28)$$

where c_2 is a universal constant.

Next, since both $\|S\| \geq 1$ and $\frac{1}{\Delta(\mathcal{T}_E)} \geq 1$, it follows that $\frac{\|S\|}{\Delta(\mathcal{T}_E)} \leq \frac{\|S\|^2}{\Delta^2(\mathcal{T}_E)}$. Thus, the term in Eq. (23) may be bounded as follows,

$$\left(\frac{\|S\|^2}{2\Delta^2(\mathcal{T}_E)} + \frac{2\|S\|}{3\Delta(\mathcal{T}_E)} \right) \leq \frac{7}{6} \frac{\|S\|^2}{\Delta^2(\mathcal{T}_E)}. \quad (29)$$

Finally, combining equations (27), (28) and (29) yields

$$\left(\frac{\|S\|^2}{2\Delta^2(\mathcal{T}_E)} + \frac{2\|S\|}{3\Delta(\mathcal{T}_E)} \right) \cdot \log \left(\frac{2m}{\epsilon} \right) \leq \begin{cases} C_1 \cdot \frac{\eta^3}{(1 - s_r^2)^2 S_{\min}^2} \cdot \log \left(\frac{m}{\epsilon} \right) & \text{if } \xi \leq \frac{1}{2}, \\ C_2 \cdot \frac{\eta^3}{(1 - s_r^2)^2 S_{\min}^2} \cdot m^{2 + 2 \log_2 \xi} \cdot \log \left(\frac{m}{\epsilon} \right) & \text{if } \xi > \frac{1}{2}. \end{cases}$$

where C_1, C_2 are absolute constants. As discussed above, this inequality yields Eq. (23). \square

H.2 Proof of Lemma 6

The proof relies on the following two auxiliary lemmas. The first is a deterministic result showing that if $\|\bar{S} - \mathbb{E}[S^g]\| \leq \Delta(\mathcal{T}_E)$, then the Fiedler vector yields a correct partition. The second is a concentration inequality on $\|\bar{S} - \mathbb{E}[S^g]\|$. Lemma 6 is proved by bounding the probability that $\|\bar{S} - \mathbb{E}[S^g]\| \geq \Delta(\mathcal{T}_E)$. We first formally state these two auxiliary results.

Lemma 8. *Let \mathcal{T}^g be a gene tree generated according to the MSC+GTR model with an underlying ultrametric species tree \mathcal{T} with m species. Let \mathcal{T}_E be the tree that corresponds to the matrix $\mathbb{E}[S^g]$, where S^g is the similarity of \mathcal{T}^g . Let $\Delta(\mathcal{T}_E)$ be the allowed error defined in Eq. (22). Then, for any symmetric matrix A*

$$\|A - \mathbb{E}[S^g]\| \leq \Delta(\mathcal{T}_E) \quad (30)$$

partitioning the terminal nodes based on the Fiedler vector of the Laplacian of A yields two clans in the species tree \mathcal{T} .

The above lemma is a variant of Lemma 5.1 from [1]. To apply the proof of [1] to our setting, we have to show that if \mathcal{T} is ultrametric, then \mathcal{T}_E is also ultrametric. This is established in Subsection H.3.

Next, we present the second result. Its proof appears in Appendix H.4.

Lemma 9 (Concentration Inequality). *Let \mathcal{T} be a species tree with m terminal nodes, and similarity matrix S . Let $\{\mathcal{T}^g\}_{g=1}^K$ be K i.i.d. gene trees generated according to the MSC+GTR model, and let $\{S^g\}_{g=1}^K$ be their exact similarity matrices. Then, the matrix $\bar{S} = \frac{1}{K} \sum_{g=1}^K S^g$ satisfies*

$$\Pr(\|\bar{S} - \mathbb{E}[S^g]\| > t) \leq 2m \exp\left(-\frac{Kt^2/2}{\|S\|^2/4 + \|S\|t/3}\right), \quad \forall t \geq 0. \quad (31)$$

We are now ready to prove Lemma 6.

Proof of Lemma 6. Let $\Delta(\mathcal{T}_E)$ be the allowed error, defined in (22). By Lemma 9, with $t = \Delta(\mathcal{T}_E)$

$$\Pr(\|\bar{S} - \mathbb{E}[S^g]\| \leq \Delta(\mathcal{T}_E)) \geq 1 - 2m \exp\left(-\frac{K\Delta^2(\mathcal{T}_E)/2}{\|S\|^2/4 + \|S\|\Delta(\mathcal{T}_E)/3}\right). \quad (32)$$

By Lemma 8, if $\|\bar{S} - \mathbb{E}[S^g]\| \leq \Delta(\mathcal{T}_E)$, the spectral partitioning is guaranteed to output a correct partition. It is easy to verify that if the number of genes K satisfies Eq. (23), then the RHS of (32) is at least $1 - \epsilon$, which concludes the proof. \square

H.3 On the proof of Lemma 8

Here we address the difference between Lemma 8 and its reference Lemma 5.1 in [1]. Both results state a condition under which the sign pattern of the Fiedler vector yields a correct partition of the leaves into two clans. Specifically, the theorems require that the input matrix for the algorithm is not too far in spectral norm from a reference matrix.

The key difference lies in the assumptions made about the trees that correspond to the reference matrices. In [1], the underlying tree \mathcal{T}_1 is assumed to be ultrametric, and its similarity is the reference matrix. In contrast, Lemma 8 assumes an ultrametric species tree \mathcal{T} , but the reference matrix is $\mathbb{E}[S^g]$, which corresponds to a different tree \mathcal{T}_E . To apply the original proof from [1], it suffices to show that \mathcal{T}_E is also ultrametric. This is formalized in the following lemma.

Lemma 10. *Let S be the similarity matrix of an ultrametric species tree \mathcal{T} . Let S^g be the similarity matrix of a gene tree \mathcal{T}^g generated according to the MSC+GTR model. Then, the tree \mathcal{T}_E with similarity $\mathbb{E}[S^g]$ is also ultrametric.*

Proof of Lemma 10. Recall that an ultrametric tree is a tree where all the leaves are at the same log-det distance from the root. Equivalently, in an ultrametric tree, the similarity between every leaf and the root is equal. We start with a property of ultrametric trees.

Let \mathcal{T} be a rooted tree with similarity S , and C_l, C_r be the two clans induced by the removal of the root. Then, easy to see that

$$\mathcal{T} \text{ is ultrametric} \iff \forall i \in C_l, j \in C_r : S_{ij} = s_0, \quad (33)$$

where s_0 is some constant.

Next, let \mathcal{T} be a species tree, S^g a gene similarity matrix generated according to the MSC+GTR model, and \mathcal{T}_E the tree corresponding to the matrix $\mathbb{E}[S^g]$. Recall \mathcal{T}_E and \mathcal{T} share the same topology, therefore C_l, C_r are clans in both trees. By Eq. (33), it suffices to show that $\mathbb{E}[S_{ij}^g] = s_0$ for all $i \in C_l, j \in C_r$.

By Eq. (33), since \mathcal{T} is ultrametric, $S_{ij} = s_1$ for all $i \in C_l$ and $j \in C_r$, for some constant s_1 . By the gene similarity under the GTR, Eq. (10), for any $i \in C_l, j \in C_r$,

$$\mathbb{E}[S_{ij}^g] = \mathbb{E}[e^{4\text{tr}(Q)\tau_{ij}^g}]$$

Inserting $\tau_{ij}^g = \tau_{ij} + \Delta_{ij}^g$, and using the definition of the species similarity, Eq. (11),

$$\mathbb{E}[S_{ij}^g] = \mathbb{E}[e^{4\text{tr}(Q)(\tau_{ij} + \Delta_{ij}^g)}] = S_{ij} \mathbb{E}[e^{4\text{tr}(Q)\Delta_{ij}^g}] = s_1 \mathbb{E}[e^{4\text{tr}(Q)\Delta_{ij}^g}].$$

It remains to claim that $\mathbb{E}[e^{4\text{tr}(Q)\Delta_{ij}^g}]$ is constant. Indeed, by the MSC model, $\{\Delta_{ij}^g\}$ are identically distributed for all $i \in C_l, j \in C_r$. \square

H.4 Proof of Lemma 9

We first present four auxiliary lemmas, used in the proof of Lemma 9. The first lemma is the Matrix Bernstein Inequality, a fundamental tool in bounding the deviation of random matrices, see [57]. The proofs of the other three lemmas appear in Appendix H.5.

Lemma 11 (Matrix Bernstein Inequality). *Let $\mathbf{A} = \sum_{l=1}^K A_l$ where A_l are independent random symmetric $m \times m$ matrices with $\mathbb{E}[A_l] = 0$ and $\|A_l\| \leq L$. Define*

$$\nu(\mathbf{A}) = \left\| \sum_{l=1}^K \mathbb{E}[A_l^2] \right\|. \quad (34)$$

Then for all $t \geq 0$,

$$\mathbb{P}(\|\mathbf{A}\| \geq t) \leq 2m \exp\left(-\frac{t^2/2}{\nu(\mathbf{A}) + Lt/3}\right). \quad (35)$$

The second lemma describes a property of the entries in the gene similarity matrix S^g .

Lemma 12. *Assuming \mathcal{T}^g is a random gene tree generated according to the MSC+GTR model, and let S^g be its similarity. Then $\forall i, j \quad 0 \leq S_{ij}^g \leq S_{ij}$.*

The third lemma describes a relation between the spectral norms of matrices with non-negative entries.

Lemma 13. *Let $A, B \in \mathbb{R}^{m \times m}$ be matrices whose entries are all non-negative. Then,*

$$\|A\| \leq \|A + B\|.$$

Let $|A|$ denote the matrix obtained by taking the entrywise absolute values of A . The fourth lemma is a basic result concerning the spectral norm of $|A|$.

Lemma 14. *Let $A \in \mathbb{R}^{m \times m}$ be a matrix. Then, $\|A\| \leq \||A|\|$.*

With those lemmas established, we present the proof. In what follows, we use the subscript A_{ij} to denote the (i, j) -th entry of a matrix A .

Proof of Lemma 9. Multiplying by K , we rewrite the probability of interest (31) as follows

$$\mathbb{P}(\|\bar{S} - \mathbb{E}[S^g]\| > t) = \mathbb{P}\left(\left\| \sum_{g=1}^K (S^g - \mathbb{E}[S^g]) \right\| > Kt\right). \quad (36)$$

Let $\mathbf{S} = \sum_{g=1}^K (S^g - \mathbb{E}[S^g])$. Since the matrices $\{S^g - \mathbb{E}[S^g]\}_{g=1}^K$ are independent and have zero mean, we can apply the Matrix Bernstein Inequality, Lemma 11 with $\mathbf{A} = \mathbf{S}$ and t replaced by Kt . Eq. (35) of this lemma depends on two quantities L and $\nu(\mathbf{S})$. To complete the proof, it remains to provide upper bounds for these two quantities.

Upper bound for L . Recall that L is an upper bound on $\|S^g - \mathbb{E}[S^g]\|$. By Lemma 12, for all $i, j \in [m]$, $S_{ij}^g \in [0, S_{ij}]$. Hence, upon subtracting the expectation, which is also in $[0, S_{ij}]$,

$$|S_{ij}^g - \mathbb{E}[S_{ij}^g]| \leq S_{ij}. \quad (37)$$

Next, we decompose S as the sum of the following two matrices:

$$S = |S^g - \mathbb{E}[S^g]| + (S - |S^g - \mathbb{E}[S^g]|),$$

By definition, all entries of the first matrix are non-negative. All entries of the second matrix are non-negative by (37). Hence, applying Lemma 13 yields,

$$\| |S^g - \mathbb{E}[S^g]| \| \leq \|S\|. \quad (38)$$

By Lemma 14 and Equation (38), we conclude that

$$\|S^g - \mathbb{E}[S^g]\| \leq \|S\|.$$

Hence, we may take $L = \|S\|$.

Upper bound for $\nu(\mathbf{S})$. Denote $V = \mathbb{E}[(S^g - \mathbb{E}[S^g])^2]$. By Equation (34), $\nu(\mathbf{S}) = K\|V\|$, hence we bound $\|V\|$. Simple computations give us:

$$|V_{ij}| = \left| \mathbb{E} \left[(S^g - \mathbb{E}[S^g])^2 \right]_{ij} \right| = \left| \sum_{l=1}^m \mathbb{E} \left[(S^g - \mathbb{E}[S^g])_{il} (S^g - \mathbb{E}[S^g])_{jl} \right] \right|.$$

By the triangle inequality, and the fact that for any two random variables X, Y , $\text{Cov}(X, Y) \leq \sigma(X)\sigma(Y)$ where $\sigma(X)$ is the standard deviation of X ,

$$|V_{ij}| \leq \sum_{l=1}^m \left| \text{Cov}(S_{il}^g, S_{jl}^g) \right| \leq \sum_{l=1}^m \sigma(S_{il}^g) \cdot \sigma(S_{jl}^g).$$

Recall that by Lemma 12, $S_{il}^g \in [0, S_{il}]$. Hence, by a well-known result for bounded random variables, $\sigma(S_{il}^g) \leq \frac{1}{2}S_{il}$ (see, e.g., [13, Chapter 2]). Therefore,

$$|V_{ij}| \leq \frac{1}{4} \sum_{l=1}^m S_{il} \cdot S_{jl} = \frac{1}{4} (S^2)_{ij}.$$

We express $\frac{1}{4}S^2$ as the sum of the following two matrices,

$$\frac{1}{4}S^2 = |V| + \left(\frac{1}{4}S^2 - |V| \right).$$

By similar arguments as above, all entries in both of these matrices are non-negative. Hence, by Lemmas 13 and 14, it follows that:

$$\|V\| \leq \| |V| \| \leq \frac{1}{4} \|S^2\|.$$

Since S is symmetric, $\|S^2\| = \|S\|^2$, together with $\nu(\mathbf{S}) = K\|V\|$, we conclude that

$$\nu(\mathbf{S}) \leq K\|S\|^2/4.$$

Inserting the above bounds on L and $\nu(\mathbf{S})$ into (35) yields the required inequality (31). \square

H.5 Proofs of auxiliary lemmas

Recall the definition from Eq. (1) of the similarity for any pair i, j of terminal nodes. Analogously, we extend this definition for any pair of nodes h, h' in the tree. To prove Lemma 7, it is useful to introduce the following vector with the similarities of all terminal nodes to their root.

Definition 4. Let r be the root of a tree \mathcal{T} with m terminal nodes. We denote by $u \in \mathbb{R}^m$ the vector of similarities from the root to each of its m leaves. Specifically, for each terminal node i ,

$$u_i = S(r, i).$$

Recall that ξ denotes the upper bound on the similarity between adjacent nodes. The following lemma bounds the l_1 norm of u .

Lemma 15. *Let \mathcal{T} be a rooted binary tree with m leaves, and let r be its root. Then,*

$$\|u\|_1 \leq \begin{cases} 1 & \text{if } \xi \leq 0.5, \\ \frac{1}{\xi} m^{1+\log_2 \xi} & \text{if } \xi > 0.5. \end{cases} \quad (39)$$

The proof of this auxiliary lemma appears below. It follows that of Lemma 4.7 in [31], which stated a lower bound on $\|u\|_2$. In what follows, we denote by S the $m \times m$ similarity matrix of the tree, and by $S(h, h')$ the similarity between the nodes h, h' .

Proof of Lemma 7. We start with a known inequality for the spectral norm

$$\|S\| \leq \sqrt{\|S\|_1 \|S\|_\infty}, \quad (40)$$

see e.g [26, Ch. 5.6, Ex. 21], where $\|\cdot\|_1, \|\cdot\|_\infty$ are the operator norms induced by the l_1 and l_∞ norms, respectively. Next, note that in general $\|A^T\|_\infty = \|A\|_1$. Since the similarity matrix S is symmetric,

$$\|S\|_1 = \|S\|_\infty. \quad (41)$$

Recall that the l_∞ operator norm of a matrix is given by the maximum l_1 norm of its rows, that is, $\|S\|_\infty = \max_i \|S_{[i,:]} \|_1$, where $S_{[i,:]}$ is the i -th row of S . Combining this with Eqs. (40), (41),

$$\|S\| \leq \max_i \|S_{[i,:]} \|_1 \quad (42)$$

We now bound $\|S_{[i,:]} \|_1$. Let r be the node attached to the i -th leaf. We denote $\mathcal{T}_r := \mathcal{T} \setminus \{i\}$ the tree obtained by removing the leaf i , and considering the node r as its root. We let $u \in \mathbb{R}^{m-1}$ be the vector of similarities of the remaining $m-1$ leaves to the node r , see Definition 4. Using the fact that the similarity function is multiplicative along paths and that $S(i, r) \leq \xi$ by the assumption in the lemma, it follows that for all $j \neq i$,

$$S(i, j) = S(i, r) \cdot S(r, j) \leq \xi \cdot u_j.$$

The row vector $S_{[i,:]}$ contains, in addition, the entry $S_{ii} = 1$. Therefore,

$$\|S_{[i,:]} \|_1 \leq 1 + \xi \cdot \|u\|_1. \quad (43)$$

Finally, combining Lemma 15 with Eqs. (43) and (42) completes the proof. \square

To complete the proof of Lemma 7, we proceed with the proof of Lemma 15.

Proof of Lemma 15. Given a rooted tree \mathcal{T} , let $u \in \mathbb{R}^m$ denote the vector of similarities from each of its m terminal nodes to the root r , see Definition 4. For each leaf i , we define its depth d_i , as the number of edges on the path from i to the root r .

By the multiplicative property of the similarity measure, u_i equals the product of the edge similarities along the path from the root to the leaf i . Given the assumption that for all pairs i, j of adjacent nodes, $S(i, j) \leq \xi$, it follows that $u_i \leq \xi^{d_i}$. Hence,

$$\|u\|_1 \leq \sum_{i=1}^m \xi^{d_i} =: B \quad (44)$$

To prove the lemma, we thus need to bound the quantity B on the RHS of (44). Note that B depends on both ξ and on the topology of the tree. To this end, for a given value of ξ , we identify the topology with the maximal value of B , as we describe now. For any tree, we define a modification in its topology. We find a topology whose value B can not be improved, and therefore it's a local maximum. We show that any other topology can be improved by the mentioned modification, thus the local maximum is unique, namely is global.

Specifically, given a candidate tree \mathcal{T} , we consider the next modification to the tree structure: We remove a pair of two terminal nodes i, j with a common neighbor, at depth $d_i = d_j$, and reattach them to a terminal node k at depth d_k . What we show next is that for $\xi \leq 0.5$ this change increases B for moving nodes from "shallow" parent node to a new "deeper" parent node, which eventually leads to a caterpillar tree. For $\xi > 0.5$, the opposite is true, leading to a balanced tree that maximizes B .

Precisely, let $\tilde{\mathcal{T}}$ be the modified tree and let \tilde{B} be its corresponding bound. The difference between \tilde{B} to B is equal to

$$\tilde{B} - B = 2\xi^{d_k+1} - 2\xi^{d_i} + \xi^{d_i-1} - \xi^{d_k}.$$

The first two terms are due to the shift of i, j from depth d_i to depth $d_k + 1$. The last two terms are due to the non-terminal node attached to i, j becoming terminal, while k becomes non-terminal. We can rewrite the last equation as:

$$\tilde{B} - B = \xi^{d_i-1}(1 - 2\xi) - \xi^{d_k}(1 - 2\xi) = (1 - 2\xi)(\xi^{d_i-1} - \xi^{d_k}) \quad (45)$$

One can see that Eq. (45) changes its behavior at $\xi = 0.5$. For $\xi \leq 0.5$, the expression in (45) is positive if $d_i - 1 < d_k$. Hence, a new tree $\tilde{\mathcal{T}}$ where the original pair of adjacent leaves of depth d_i is now at depth $d_k + 1$, where $d_k + 1 > d_i$, has a larger value \tilde{B} . Repeating this step increases the norm until such changes are no longer possible. The extreme case is the tree that contains exactly one terminal node at depth d_l for $d_l = 1, \dots, m - 2$, and two terminal nodes at depth $m - 1$, that is, the caterpillar tree.

For $\xi > 0.5$, the argument is analogous. In this case, the expression in (45) is positive if $d_i - 1 > d_k$. Thus, moving x_1, x_2 from depth d_i to depth $d_k + 1$ increases B . As in the previous case, we repeatedly apply this modification until we reach the extremal topology - in this case, the perfectly balanced tree, when $m = 2^n$ for some $n \in \mathbb{N}$. If $m \neq 2^n$, then the extremal topology can be described as follows. Define the l -th level of a binary rooted tree \mathcal{T} to be the set of nodes at depth l . A level l is said to be *full* if it contains exactly 2^l nodes. With this terminology in place, the extremal topology is a binary tree in which all levels up to $\lfloor \log_2 m \rfloor$ are full, and the remaining leaves are placed at depth $\lfloor \log_2 m \rfloor + 1$.

We now compute B for each of the two extreme cases. For the caterpillar tree,

$$B = \sum_{l=1}^{m-1} \xi^l + \xi^{m-1} = \frac{\xi}{1-\xi} (1 - \xi^{m-1}) + \xi^{m-1}.$$

For $\xi \leq 0.5$, since $\xi/(1-\xi) \leq 1$ then

$$\frac{\xi}{1-\xi} (1 - \xi^{m-1}) + \xi^{m-1} \leq 1 - \xi^{m-1} + \xi^{m-1} = 1.$$

For the balanced tree, let N be the number of nodes at the non-full level, which is $\lfloor \log_2 m \rfloor + 1$, e.g, for $m = 2^n$, N equals zero. Hence

$$B = N\xi^{\lfloor \log_2 m \rfloor + 1} + (m - N)\xi^{\lfloor \log_2 m \rfloor} = (N\xi + (m - N))\xi^{\lfloor \log_2 m \rfloor} = (N\xi + (m - N))\frac{1}{\xi}\xi^{\lfloor \log_2 m \rfloor + 1}$$

Since, $\lfloor \log_2 m \rfloor + 1 > \log m$ and $\xi < 1$ we can bound from above as follows,

$$B \leq \frac{m}{\xi} \xi^{\log_2 m} = \frac{1}{\xi} m^{1 + \log_2 \xi},$$

where the second equality follows from basic logarithmic identities,

$$\xi^{\log_2 m} = m^{\log_m(\xi^{\log_2 m})} = m^{\log_2 m \cdot \log_m \xi} = m^{\log_2 m \cdot \frac{\log_2 \xi}{\log_2 m}} = m^{\log_2 \xi}.$$

This concludes the proof. □

Proof of Lemma 12. Using the expression for S_{ij}^g in Eq. (10), the definition of Δ_{ij}^g , and S_{ij} ,

$$S_{ij}^g = \exp(4\text{tr}(Q)\tau_{ij}^g) = \exp(4\text{tr}(Q)(\tau_{ij} + \Delta_{ij}^g)) = S_{ij} \exp(4\text{tr}(Q)\Delta_{ij}^g).$$

Since Δ_{ij}^g is non negative random variable, and $\text{tr}(Q) < 0$, it follows that $\exp(4\text{tr}(Q)\Delta_{ij}^g)$ is supported on $[0,1]$. \square

Recall that for a vector v or a matrix A , $|v|$ and $|A|$ denote the vector or matrix obtained by taking the absolute value entry-wise.

Proof of Lemma 13. Let $v \in \mathbb{R}^m$ be a unit vector such that $\|A\| = \|Av\|$. Since A has non-negative entries, we may assume that all entries of v are non-negative. Indeed, if some entries of v are negative, define a new vector $u \in \mathbb{R}^m$ by $u_i = |v_i|$. Clearly, $\|u\| = \|v\| = 1$, and since $A \geq 0$ entrywise, it follows that $Au \geq |Av| \geq 0$ entrywise, and hence $\|Au\| \geq \|Av\|$. If the inequality is strict, this contradicts the maximality of $\|Av\|$; otherwise, we may replace v with u .

Next, observe that since both A and B are entrywise non-negative, the vectors Av and Bv are also non-negative. Hence:

$$\|A\| = \|Av\| \leq \|Av + Bv\| = \|(A + B)v\| \leq \|A + B\|.$$

\square

Proof of Lemma 14. Let A be an $m \times m$ matrix, and let $v \in \mathbb{R}^m, u \in \mathbb{R}^m$ be defined as in the proof of Lemma 13 above. Using the definition of the spectral norm, of the vector v , and the fact that $\|w\| = \||w|\|$ for any vector w ,

$$\|A\| = \|Av\| = \||Av|\| \tag{46}$$

Next, we turn to upper bound the i th entry of $|Av|$. By the triangle inequality,

$$|(Av)_i| = \left| \sum_{j=1}^m A_{ij}v_j \right| \leq \sum_{j=1}^m |A_{ij}| |v_j| = (|A|u)_i.$$

Hence,

$$\||Av|\| \leq \||A|u\| \leq \||A|\|. \tag{47}$$

Combining Eqs. (46) and (47), completes the proof. \square

50 Species Datasets - Single Iteration

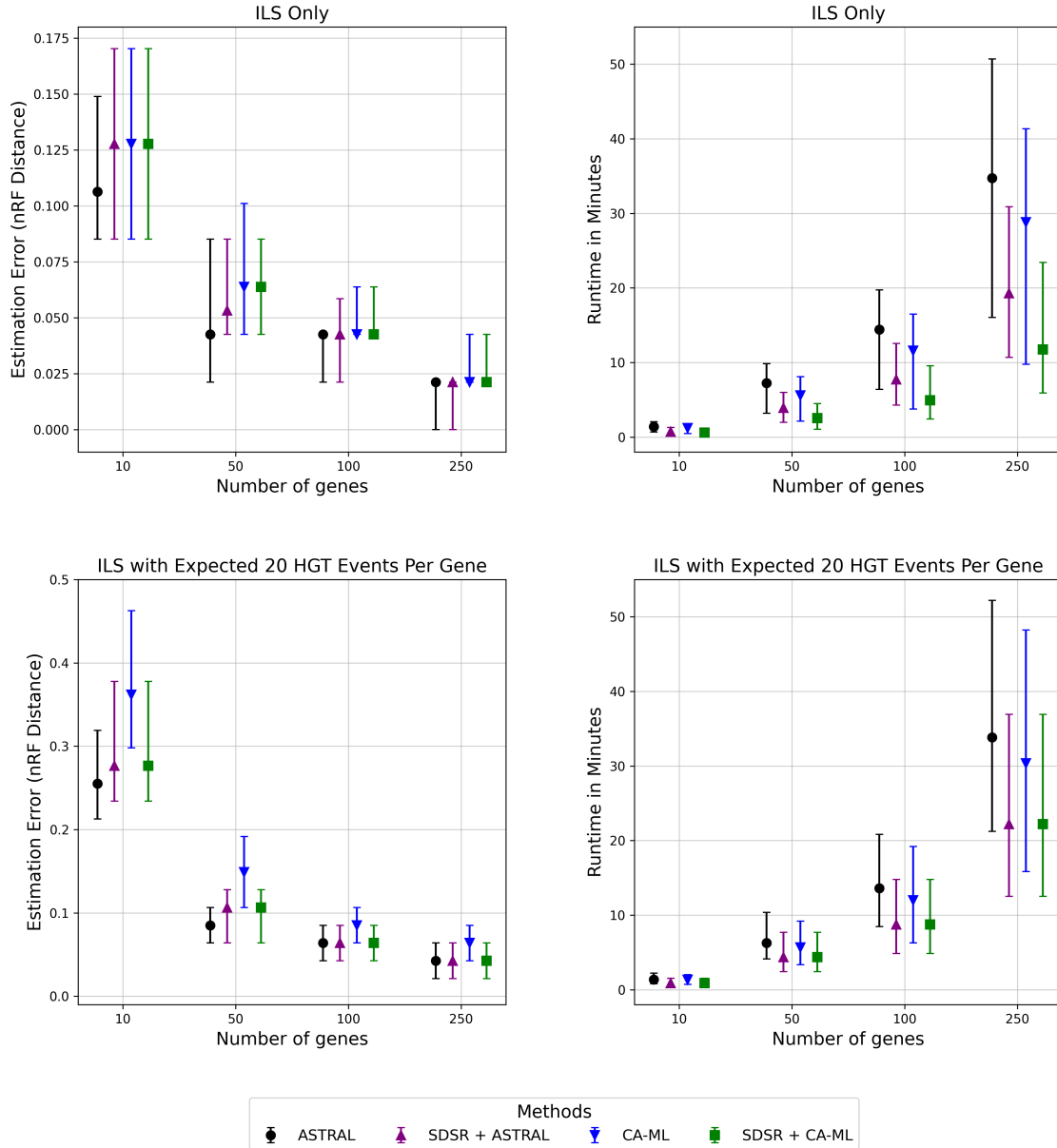


Figure 11: Results for the 50 species datasets with a single SDRS iteration: The left panels show the nRF distance between the estimated and ground-truth species trees as a function of the number of genes, for the dataset with only ILS (upper panel) and ILS+HGT (bottom panel). The right panels show the runtime in minutes.

200 Species Datasets - Single Iteration

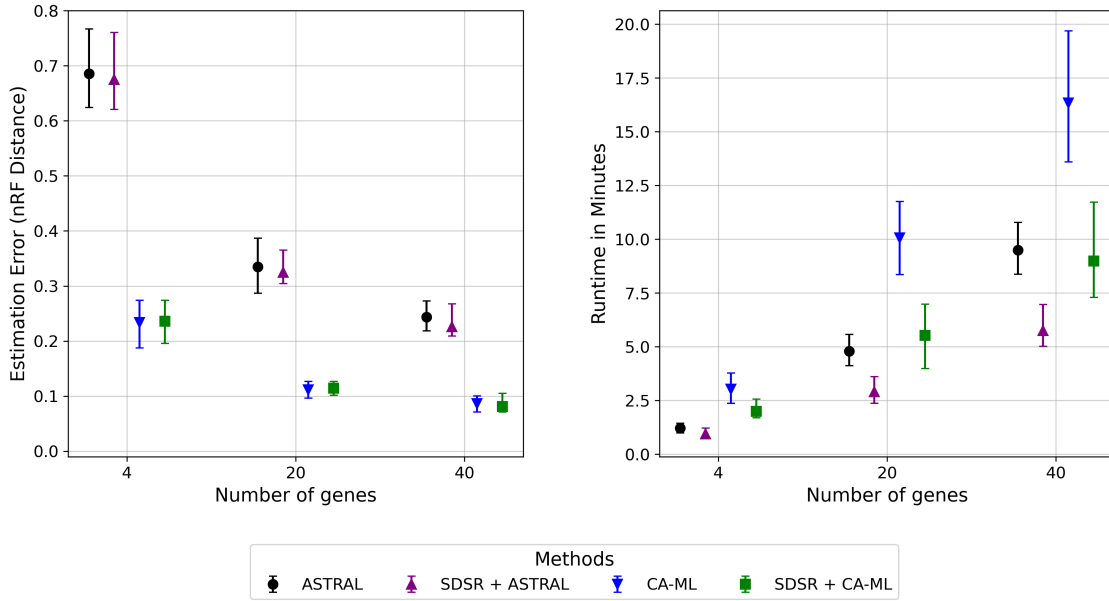


Figure 12: Results for the 200 species datasets with a single SDRS iteration: (left panel) nRF distance between the estimated and ground-truth species trees as a function of the number of genes; (right panel) runtime in minutes.

200 Species Datasets - Different Recursion Levels

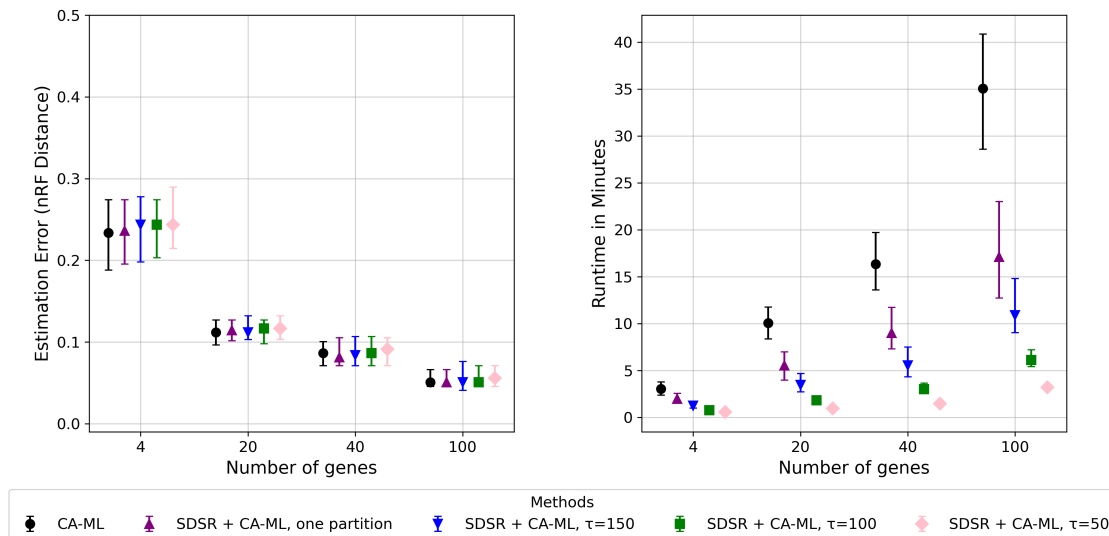


Figure 13: Results for the 200 species datasets - multiple SDRS iterations on a single CPU: (left panel) nRF distance between the estimated and ground-truth species trees as a function of the number of genes; (right panel) runtime in minutes.